Caspar, AT, Helfer, AG, Michely, JA, Auwaerter, V, Brandt, SD, Meyer, MR and Maurer, HH

Studies on the metabolism and toxicological detection of the new psychoactive designer drug 2-(4-iodo-2,5-dimethoxyphenyl)-N-[(2-methoxyphenyl)methyl]ethanamine (25I-NBOMe) in human and rat urine using GC-MS, LC-MSn, and LC-HR-MS/MS

Analytical & Bioanalytical Chemistry

Studies on the metabolism and toxicological detection of the new psychoactive designer drug 2-(4-iodo-2,5-dimethoxyphenyl)-N-[(2-methoxyphenyl)methyl]ethanamine (25I-NBOMe) in human and rat urine using GC-MS, LC-MSn, and LC-HR-MS/MS

Journal:	*Analytical and Bioanalytical Chemistry*
Manuscript ID:	Draft
Type of Paper:	Research Paper
Date Submitted by the Author:	n/a
Complete List of Authors:	Caspar, Achim; Saarland University, Dept. of Experimental & Clinical Toxicology Helfer, Andreas; Saarland University, Dept. of Experimental & Clinical Toxicology Michely, Julian; Saarland University, Dept. of Experimental & Clinical Toxicology Auwärter, Volker; Institute of Forensic Medicine, Forensic Toxicology BRANDT, SIMON; Liverpool John Moores University, School of Pharmacy and Biomolecular Sciences Meyer, Markus; Saarland University, Department of Experimental and Clinical Toxicology Maurer, Hans; Saarland University, Department of Experimental and Clinical Toxicology
Keywords:	Bioanalytical methods, Drug monitoring / Drug screening, Forensics / Toxicology, Mass spectrometry / ICP-MS

Studies on the metabolism and toxicological detection of the new psychoactive designer drug 2-(4-iodo-2,5-dimethoxyphenyl)-*N*-[(2-methoxyphenyl)methyl]ethanamine (25I-NBOMe) in human and rat urine using GC-MS, LC-MS^n, and LC-HR-MS/MS

Achim T. Caspar * Andreas G. Helfer * Julian A. Michely * Volker Auwärter * Simon D. Brandt * Markus R. Meyer * Hans H. Maurer

---

Achim T. Caspar * Andreas G. Helfer * Julian A. Michely * Markus R. Meyer * Hans H. Maurer (corresponding author)

Department of Experimental and Clinical Toxicology, Institute of Experimental and Clinical Pharmacology and Toxicology, Saarland University, D-66421 Homburg (Saar), Germany

E-Mail: hans.maurer@uks.eu

Volker Auwärter

Institute of Forensic Medicine, Forensic Toxicology, Medical Center - University of Freiburg, D-79104 Freiburg, Germany

Simon D. Brandt

School of Pharmacy and Biomolecular Sciences, Liverpool John Moores University, James Parsons Building, Byrom Street, Liverpool L3 3AF, UK

Markus R. Meyer

Present address: Farmakologiska laboratoriet, Klinisk farmakologi, Karolinska Universitetssjukhuset Huddinge, Karolinska Institutet, 141 86 Stockholm, Sweden

Abstract

25I-NBOMe, a new psychoactive substance, is a potent 5-HT_{2A} receptor agonist with strong hallucinogenic potential. Recently, it was involved in several fatal and non-fatal intoxication cases. The aim of the present work was to study its phase I and II metabolism and its detectability in urine screening approaches. After application of 25I-NBOMe to male Wistar rats, urine was collected over 24h. The phase I and II metabolites were identified by LC-HR-MS/MS in urine after suitable workup. For the detectability studies, standard urine screening approaches (SUSA) by GC-MS, LC-MS^n, and LC-HR-MS/MS were applied to rat and also to authentic human urine samples submitted for toxicological analysis. Finally, an initial CYP activity screening was performed to identify CYP isoenzymes involved in the major metabolic steps. 25I-NBOMe was mainly metabolized by *O*-demethylation, *O,O-bis*-demethylation, hydroxylation, and combinations of these reactions as well as by glucuronidation and sulfation of the main phase I metabolites. All in all, 68 metabolites could be identified. Intake of 25I-NBOMe was detectable mainly via its metabolites by both LC-MS approaches, but not by the GC-MS SUSA. Initial CYP activity screening revealed the involvement of CYP1A2 and CYP3A4 in hydroxylation and CYP2C9 and CYP2C19 in *O*-demethylation. The presented study demonstrated that 25I-NBOMe was extensively metabolized and could be detected only by the LC-MS screening approaches. Since CYP2C9 and CYP3A4 are involved in initial metabolic steps, drug-drug interactions might occur in certain constellations.

Keywords: designer drugs; 25I-NBOMe; metabolism; cytochrome-P450; LC-MS^n; LC-HR-MS/MS

Introduction

In recent years, with *N*-2-methoxybenzyl phenethylamine (NBOMe) derivatives a new class of so-called New Psychoactive Substances (NPS) appeared on the drug scene. They are derived from a class of the well-known potent hallucinogenic phenethylamines, the so-called 2Cs [1]. The NBOMe derivatives are very potent serotonin receptor agonists as figured out in structure-activity relationship studies [2, 3]. Thus, they have a high potential for hallucinogenic effects with the risk of serotonergic toxicity. Among others, 2-(4-bromo-2,5-dimethoxyphenyl)-*N*-[(2-methoxyphenyl)methyl]ethanamine (25B-NBOMe, 2C-B-NBOMe), 2-(4-chloro-2,5-dimethoxyphenyl)-*N*-[(2-methoxyphenyl)methyl]ethanamine (25C-NBOMe, 2C-C-NBOMe), and 2-(4-iodo-2,5-dimethoxyphenyl)-*N*-[(2-methoxyphenyl)methyl]ethanamine (25I-NBOMe, 2C-I-NBOMe) have been sold and consumed as so-called research chemicals. For example, 25I-NBOMe is usually consumed in form of blotter papers, powder, or as nose sprays at very low doses of 0.5-1.5 mg (https://www.erowid.org). In the meantime, most of them have been scheduled in many countries considering the common use and partly fatal poisoning cases [4-9]. In such cases, the drugs must be screened and quantified in clinical and forensic laboratories. Several procedures for quantification of NBOMe's in serum specimen have been published [4, 10], but if the consumed drugs are unknown, screening procedures, mostly in urine, are initially applied. One requisite for developing screening approaches reliably detecting such lipophilic drugs is to know the analytical targets in body samples [11-13]. Thus, the metabolism should be studied first. This is also relevant for assessing of drug-drug interactions or toxic risks. Such studies have been comprehensively performed for the underlying 2C analogues [14-21]. However, there is no systematic study available on the metabolism or detectability in urine of NBOMe derivatives. Among the NBOMe derivatives, 25I-NBOMe seems to be the most commonly used drug. Stellpflug et al. [7] described the possible presence of three *O*-demethyl- isomers but no detailed metabolism studies were done. Therefore, the aim of the present study was to elucidate the metabolism of 25I-NBOMe in rats and humans using Orbitrap (OT)-based LC-HR-MS/MS. Furthermore, the detectability of 25I-NBOMe

and its metabolites by the authors' standard urine screening approaches (SUSA) by GC-MS [22], LC-MS^n [23], or LC-HR-MS/MS (Helfer et al., submitted) should be studied.

Experimental

Chemicals and reagents

25I-NBOMe hydrochloride was purchased by LGC Standards (Wesel, Germany). Isolute HCX cartridges (130 mg, 3 mL) were obtained from Biotage (Uppsala, Sweden), isocitrate and isocitrate dehydrogenase from Sigma (Taufkirchen, Germany), $NADP^+$ from Biomol (Hamburg, Germany), acetonitrile (LC-MS grade), ammonium formate (analytical grade), formic acid (LC-MS grade), methanol (LC-MS grade), mixture (100,000 Fishman units/mL) of glucuronidase (EC No. 3.2.1.31) and arylsulfatase (EC No. 3.1.6.1) from *Helix Pomatia*, and all other chemicals and reagents (analytical grade) from VWR (Darmstadt, Germany). The baculovirus-infected insect cell microsomes (Supersomes) containing 1 nmol/mL of human cDNA-expressed CYP1A2, CYP2A6, CYP2B6, CYP2C8, CYP2C9, CYP2C19, CYP2D6, CYP2E1 (2 nmol/mL), CYP3A4, or CYP3A5 (2 nmol/mL), and pooled human liver microsomes (pHLM, 20 mg microsomal protein/mL, 400 pmol total CYP/mg protein) were obtained from BD Biosciences (Heidelberg, Germany). After delivery, the microsomes were thawed at 37°C, aliquoted, snap-frozen in liquid nitrogen, and stored at -80°C until use.

Urine samples

According to the usual study design [24], the investigations were performed using rat urine samples from male Wistar rats (Charles River, Sulzfeld, Germany) for toxicological diagnostic reasons according to the corresponding German law. The compound was administered in an aqueous

suspension by gastric intubation of a single 4 mg/kg body weight (BW) dose for identification of the metabolites and of 0.05 and 0.1 mg/kg BW) for screening. The rats were housed in metabolism cages for 24 h, having water *ad libitum*. Urine was collected separately from the feces over a 24 h period. Blank urine samples were collected before drug administration to check whether the samples were free of interfering compounds. The samples were directly analyzed and then stored at -20°C.

An authentic human urine sample after unintentional intake of 25I-NBOMe submitted to the authors' laboratory for toxicological diagnostics was also analyzed.

Sample preparation for identification of phase I metabolites by LC-HR-MS/MS

According to published procedures [24], 2 mL of urine was adjusted to pH 5.2 with acetic acid (1 M, approximately 50 µL) and incubated at 56 °C for 2 h with 50 µL of a mixture of glucuronidase and arylsulfatase. The urine sample was then loaded on an HCX cartridge previously conditioned with 1 mL of methanol and 1 mL of water. After passage of the sample, the cartridge was washed with 1 mL of water, 1 mL of 0.01 M hydrochloric acid, and again with 1 mL of water. The acidic and neutral compounds (eluate A) were eluted with 1 mL of methanol into a 1.5 mL reaction vial and the basic compounds (eluate B) with 1 mL of a freshly prepared mixture of methanol/aqueous ammonia 32% (98:2, *v/v*), respectively. The eluates were evaporated to dryness under a stream of nitrogen and reconstituted with 50 µL of a mixture of eluent A and B (1:1, *v/v*) for LC-HR-MS/MS analysis. A 10-µL aliquot of each extract was then injected onto the LC-HR-MS/MS.

Sample preparation for identification of phase II metabolites by LC-HR-MS/MS

According to published procedures [24], 100 µL of urine was mixed with 500 µL of acetonitrile for precipitation. After shaking and centrifugation, the supernatant was gently evaporated to dryness

and reconstituted in 50 µL of a mixture of 10 mM aqueous ammonium formate buffer (pH 3) and acetonitrile (1:1, *v/v*) and 10 µL injected onto the LC-HR-MS/MS system.

Microsomal incubations for initial CYP activity screening studies

According to standard procedures [24, 25], microsomal incubations were performed at 37°C at a concentration of 25 µM 25I-NBOMe with the CYP isoenzymes (75 pmol/mL, each) CYP1A2, CYP2A6, CYP2B6, CYP2C8, CYP2C9, CYP2C19, CYP2D6, CYP2E1, CYP3A4, or CYP3A5 for 30 min as well as HLM (20 mg protein/mL) as positive control. Besides enzymes and substrates, the incubation mixtures (final volume, 50 µL) contained 90 mM phosphate buffer (pH 7.4), 5 mM Mg^{2+}, 5 mM isocitrate, 1.2 mM $NADP^{+}$, 0.5 U/mL isocitrate dehydrogenase, and 200 U/mL superoxide dismutase. For incubations with CYP2A6 or CYP2C9, phosphate buffer was replaced with 45 mM and 90 mM Tris buffer, respectively, according to the Gentest manual. Reactions were initiated by addition of the microsomes and stopped with 50 µL of ice-cold acetonitrile, containing 5 µM trimipramine-d_3 as internal standard. The solution was centrifuged for 2 min at 14,000×g; 70 µL of the supernatant phase were transferred to an autosampler vial and 10 µL injected onto the LC-HR-MS/MS system.

LC-HR-MS/MS apparatus for identification of phase I and II metabolites and CYP initial screening

According to published procedures [26], the extracts were analyzed using a ThermoFisher Scientific (TF, Dreieich, Germany) Accela LC system consisting of a degasser, a quaternary pump and an HTC PAL Autosampler (CTC Analytics AG, Zwingen, Switzerland), coupled to a TF Q-Exactive system equipped with a heated electrospray ionization (HESI)-II source. The instrument was used in positive ionization mode or in positive/negative switching mode. Mass calibration was

done prior to analysis according to the manufacturer's recommendations using external mass calibration.

Gradient elution was performed on a TF Accucore PhenylHexyl column (100 mm x 2.1 mm, 2.6 µm). The mobile phases consisted of 2 mM aqueous ammonium formate containing formic acid (0.1%, *v*/*v*) and acetonitrile (1%, *v*/*v*) (pH 3, eluent A) and ammonium formate solution with acetonitrile:methanol (50:50, *v*/*v*) containing formic acid (0.1%, *v*/*v*) and water (1%, *v*/*v*) (eluent B). The gradient and flow rate were programmed as follows: 0-1 min hold 1% B, 1-16 min 5% B to 95% B, 16-18 min hold 95% B, and 18-20 min hold 1% B, constantly at 500 µL/min.

The HESI-II source conditions were as follows: sheath gas, 60 arbitrary units (AU); auxiliary gas, 10 AU; spray voltage, 3.00 (positive polarity) and -4.00 kV (negative polarity); heater temperature, 320°C; ion transfer capillary temperature, 320°C; and S-lens RF level, 60.0. Mass spectrometry was performed in positive polarity mode for the eluate B and in positive/negative polarity switch mode for the eluate A using full scan (FS) data and a subsequent data dependent acquisition (DDA) mode with an inclusion list on the masses of the metabolites.

The settings for FS data acquisition were as follows: resolution, 35,000; microscans, 1; automatic gain control (AGC) target, 1e6; maximum injection time (IT), 120 ms; and scan range, m/z 70 – 1000. The settings for the DDA mode (loop count 5) with an inclusion list for the expected metabolites were as follows: precursor ions, transferred to an exclusion list for 1 s (dynamic exclusion); resolution, 17,500; microscans, 1; AGC target, 2e5; maximum IT, 250 ms; isolation window, 1.0 *m/z*; HCD with stepped normalized collision energy (NCE), 17.5, 35, and 52.5%; spectrum data type, profile; and underfill ratio, 0.1%.

For analyzing the initial CYP activity screening, the MS settings and the mobile phases were the same. The inclusion list only contained the masses of corresponding metabolites (*m/z* 308.0148, 414.0561, and 444.0666). The gradient and flow rate were as follows: 0-0.5 min hold 20% B, 0.5-2.5 min 20% B to 50% B, 2.5-4 min hold 50% B, 4-5.5 min 50% B to 80%, 5.5-6 min hold 80% B, and 6-7 min hold 20% B, constantly at 500 µl/min.

GC-MS SUSA

The GC-MS SUSA was performed as described elsewhere [22].

LC-MS^n SUSA

In accordance to Wissenbach et al. [23, 27], the urine samples (100 µL) were worked up by precipitation as described for the identification of phase II metabolites. The samples were separated and analyzed using a TF LXQ linear ion trap MS equipped with a HESI II source and coupled to a TF Accela LC system consisting of a degasser, a quaternary pump, and an autosampler. Gradient elution was performed using a TF Hypersil Gold (150 x 2.1 mm, 1.9 µm) column and 10 mM aqueous ammonium formate buffer containing formic acid (0.1%, *v/v*) as mobile phase A and acetonitrile containing formic acid (0.1%, *v/v*) as mobile phase B. The gradient and flow rate were programmed from 98% to 0% A at 500 µL/min within 21 min (injection volume 10 µL). DDA was conducted on precursor ions selected from MS^1. MS^1 was performed in FS mode (*m/z* 100-800). MS^2 and MS^3 were performed in DDA mode: four DDA MS^2 scan filters were chosen to provide MS^2 on the four most intense signals from MS^1 and additionally, eight MS^3 scan filters were chosen to record MS^3 on the most and second most intense signals from the MS^2. MS^2 spectra were collected with a higher priority than MS^3 spectra. Wideband NCE with collision induced dissociation were 35% for MS^2 and 40% for MS^3.

TF ToxID 2.1.1 was used for automatic target screening in the MS^2 screening mode. The settings were as follows: retention time (RT) window, 20 min; RT, 0.1 min; signal threshold, 100 counts; search index, 600; reverse search index, 700. ToxID was run automatically after file acquisition using an Xcalibur processing method starting both software tools [28]. The MS^2 and MS^3 reference spectra were recorded in urine after the above-mentioned workup and analysis. They were confirmed by comparison with the corresponding LC-HR-MS/MS spectra.

LC-HR-MS/MS SUSA

According to Helfer et al. (manuscript submitted), the same LC-HR-MS/MS apparatus was used as for the identification of phase I and II metabolites with gradient elution on a TF Accucore PhenylHexyl column (100 x 2.1 mm, 2.6 µm). The mobile phases consisted of 2 mM aqueous ammonium formate containing formic acid (0.1%, *v*/*v*) (pH 3, eluent A) and ammonium formate solution with acetonitrile:methanol (50:50, *v*/*v*) containing formic acid (0.1%, *v*/*v*) and water (1%, *v*/*v*) (eluent B). The flow rate was set to 500 µL/min for 10 min and 800 µL/min from 10-13.5 min and the gradient was programmed as follows: 0-1.0 min 1% B, 1-10 min to 99% B, 10-11.5 min hold 99% B, 11.5-13.5 min hold 1% B. The HESI-II source conditions were as described above, but with a scan range of *m/z* 130-1000.

For DDA, High Energy Collisional Dissociation (HCD) experiments were performed on the five most intense precursor ions selected from FS using DDA (loop count 5). The five most intense precursor ions were transferred to an exclusion list for 8 s, defined by the term dynamic exclusion. The remaining settings for DDA mode were as follows: resolution, 17,500; microscans 1, AGC target, 2e5; maximum IT, 250 ms; isolation window, 1.0 *m/z*, HCD with stepped NCE, 17.5, 35, and 52.5%, spectrum data type, profile, and underfill ratio, 0.5%.

For identification (I), the accurate precursor ion must be detectable and the underlying HR-MS/MS spectrum must fit with the reference library spectrum. For Detection (D), only the accurate precursor ion must be detectable. This classification was in accordance to that described by Broecker et al. [29].

Results and discussion

HR-MS/MS fragmentation and identification of 25I-NBOMe and its phase I metabolites

Thirty seven phase I metabolites could be identified. Therefore, besides the MS^2 spectra of 25I-NBOMe only those representing typical pathways are depicted in Fig. 1 and discussed in detail here. A list of all phase I metabolites is given in Table 1. The precursor masses (PM) are given with the calculated exact masses. The 4-iodo-2,5-dimethoxyphenethylamine partial structure of the parent compound will be referred as 2C part on the following pages. Fragmentation patterns will be discussed of representatives for each metabolic reactions leading to different fragmentation.

25I-NBOMe (**1** in Fig. 1 and Table 1; PM at *m/z* 428.0717, M+H) showed a fragmentation pattern, characteristic also for most of the detected metabolites. The most abundant fragment ion (FI) in MS^2 at *m/z* 121.0653 represented the cleavage of the methoxybenzyl moiety, followed by the loss of the methoxy group (-30.0105 u) producing the tropylium ion at *m/z* 91.0548. The FI representing the 2C part showed a low abundance of less than 3 % (inserts of the corresponding spectra in Fig. 1). The FI at *m/z* 305.9991 representing the 2C iminium ion resulted from benzyl cleavage. A loss of NH (- 15.0109 u) formed the FI at *m/z* 290.9882 followed by a loss of a methyl radical (- 15.0235 u) of one of the two methoxy groups in the 2C part resulting in FI at *m/z* 275.9647. The FI at *m/z* 301.1678 ($C_{18}H_{23}O_3N$) resulted from a loss of iodine as a radical. One FI at *m/z* 272.1407 ($C_{17}H_{20}O_3$) could not result from a cleavage of the unchanged parent compound (loss of CH_3NI). In absence of other plausible explanations, a rearrangement reaction of the parent compound was postulated (Fig. 2). This rearrangement might be explained by an intramolecular electrophilic attack of the benzyl carbon at position 3, 4, or 6 of the 2C ring system, which was activated by the +M effects of the two methoxy groups and the iodine atom and by the +I effect of the alkyl chain. After elimination of HI and $NH{=}CH_2$ this led to the FI at *m/z* 272.1407 ($C_{17}H_{20}O_3$).

The MS^2 spectra of the *N*-demethoxybenzyl metabolite (2C-I, **5**, PM at *m/z* 308.0148, M+H) showed a most abundant FI at *m/z* 290.9882 representing a shift of ammonia (- 17.0266 u). As described above, a loss of a methyl radical (-15.0235 u) formed the FI at *m/z* 275.9647. In the parent compound spectrum, the same fragments were found without the postulated rearrangement reaction. This metabolite could be further confirmed by comparison with reference material.

N-demethoxybenzylation in combination with *O*-demethylation led to two isomers of *N*-demethoxybenzyl-*O*-demethyl 25I-NBOMe (**2** and **3**, PM at *m/z* 293.9991, M+H). Both showed more or less the same fragmentation pattern (*m/z* 261.9491 and 276.9726) and an exact prediction, which methoxy group was demethylated, cannot be done. This was marked by a tilde bond in the structures (Figs. 1-4). The fragmentation corresponds to the *N*-demethoxybenzyl metabolite (**5**) with a loss of one methyl group (- 15.0235 u).

The spectra of *O*-demethyl metabolites (**12** and **14**) showed a PM at *m/z* 414.0561 (M+H) with the elemental composition of $C_{17}H_{21}O_3NI$. The FIs at *m/z* 91.0548 and 121.0653 represented the unchanged methoxybenzyl moiety and indicated *O*-demethylation at the 2C part. The FIs at *m/z* 276.9726 and 291.9835 corresponded to those of the parent compound with demethylation at one of the two methoxy groups (**12**). This metabolite showed FIs indicating the postulated rearrangement reaction as described for the parent compound. The FI at *m/z* 397.0301 ($C_{17}H_{18}O_3I$) resulted from a loss of ammonia (- 17.0266 u) of the precursor, which could occur in the course of the postulated rearrangement reaction. Further products are the FIs at *m/z* 270.1256 and 287.1521 representing the rearrangement products of the de-iodinated precursor followed by elimination of ammonia. The other *O*-demethyl metabolite (**14,** PM at *m/z* 414.0561, M+H) showed different fragmentation patterns. The shift of the FI at *m/z* 121.0653 (**12**, unchanged methoxybenzyl moiety) to *m/z* 107.0497 resulted from a loss of the methyl group of the methoxybenzyl moiety. In contrast to the parent compound, the 2C part showed a FI at *m/z* 308.0148 indicating a primary amine (as described for the *N*-demethoxybenzyl metabolite, **5**) and not an iminium ion. The following fragmentation patterns were similar to those of the parent compound. The FIs of the 2C part were the same as already described for the *N*-demethoxybenzyl metabolite (**5**). The relative abundance of the 2C FIs was much higher than those seen for the parent compound spectra, which might be explained by a hydrogen bond between the resulting hydroxy group of the methoxybenzyl moiety and the nitrogen atom of the 2C part. This hydrogen bond might stabilize the molecule explaining why this metabolite did not show any FIs corresponding to the already described rearrangement reaction. Furthermore, this hydrogen bond led to another fragment of the 2C part compared to the

non *O*-demethylated methoxybenzyl moiety. Instead of the resulting iminium ion (**1**, *m/z* 305.9991), a primary amine was formed (*m/z* 308.0148). This fragmentation pattern could be seen for all metabolites with an *O*-demethylation at the methoxybenzyl moiety.

Hydroxylation took place at different positions (**32**, **34,** and **35**; PM at *m/z* 444.0666, M+H). Isomer 1 (**32**) showed the fragments of the unchanged methoxybenzyl moiety (*m/z* 91.0548 and 121.0653) indicating hydroxylation at the 2C part (*m/z* 306.9831). As no fragments for loss of water were observed, hydroxylation at the aryl ring system could be assumed. Isomer 4 (**35**) did also form FI at *m/z* 306.9831, but the FI at *m/z* 426.0561 representing loss of water (- 18.0100 u) indicated hydroxylation at the alkyl chain at an unknown position. Metabolic and/or artificial dehydration led to dehydro 25I-NBOMe (**22**, PM at *m/z* 426.0561, M+H; spectrum not shown). The most abundant FIs at *m/z* 91.0548 and 121.0653 represented the unchanged methoxybenzyl moiety, so the double bond might be located in the 2C part. The position of the double bond might be between the alpha carbon and the nitrogen forming an imine (25I-NBOMe imine analog [5]). The FIs of the 2C part were different. The FI at *m/z* 303.9835 representing the 2C nitrilium ion resulted from the benzyl cleavage. In contrast to the compound spectra this fragment did not show a loss of ammonia. The loss of iodine radical from the precursor led to the FI at *m/z* 299.1521. This metabolite did not show any FIs for the postulated rearrangement reaction. Finally, isomer 3 (**34**) showed a FI at *m/z* 137.0603 resulting from a hydroxylation at the methoxybenzyl moiety and FIs at *m/z* 275.9647 and 290.9882 representing the unchanged 2C part as described above.

The fragmentation patterns of metabolites hydroxylated at the methoxybenzyl moiety and *O*-demethylated at both parts (**26** and **28**; PM at *m/z* 430.0510, M+H) corresponded to the respective *O*-demethyl (**12** and **14**) or hydroxy (**34**) metabolite. Isomer 2 (**26**) showed FIs at *m/z* 137.0603 and 276.9726 representing hydroxylation at the methoxybenzyl moiety and *O*-demethylation at the 2C part. The exact position of the hydroxylation and *O*-demethylation could not be predicted. Isomer 4 (**28)** showed FIs of the unchanged 2C part (*m/z* 290.9882 and 308.0148). Metabolic *O*-demethylation (- 14.0157 u) and hydroxylation (+ 15.9950 u) at the methoxybenzyl moiety (*m/z* 121.0653) led to *m/z* 123.0446.

HR-MS/MS fragmentation and identification of the phase II metabolites

Thirty phase II metabolites could be identified and selected spectra representing the various pathways are depicted in Fig. 3. A list of all phase II metabolites is given in Table 2. All glucuronides eliminated glucuronic acid (- 176.0321 u) and all sulfates sulfuric acid (- 79.9568 u). For example, the glucuronidated *O*-demethyl metabolite (**58**, PM at *m/z* 590.0882, M+H) eliminated glucuronic acid and thus, the rest of the spectrum corresponded to that of the *O*-demethyl metabolite (**14**, Fig. 1). Further fragments were formed of partial structures containing the glucuronic or sulfuric acid rests. These allowed elucidation at which part of the molecule conjugation took place. For the *O,O-bis*-demethyl metabolite (**8**, PM at *m/z* 400.0404, M+H, spectrum not shown), two different sulfation products (**48** and **49**, PM at *m/z* 479.9972, M+H) could be detected with different fragmentation patterns. In the spectrum of isomer 2 (**48**) the FIs at *m/z* 356.9294 and 373.9556 represented sulfation at the 2C part. In contrast, isomer 3 (**49**) showed FI at *m/z* 204.0331 representing sulfation at the methoxybenzyl moiety. The spectrum of the glucuronidated *O,O-bis*-demethyl metabolite (**54**, PM at *m/z* 576.0725, M+H) showed a FI at *m/z* 470.0312 representing glucuronidation at the 2C part. The glucuronide of the hydroxy metabolite isomer 3 (**69**, PM at *m/z* 620.0987, M+H) formed a FI at *m/z* 313.0923 confirming glucuronidation of the metabolite hydroxylated at the methoxybenzyl moiety. The glucuronide of the *O,O-bis*-demethyl-hydroxy metabolite (**60**, PM at *m/z* 592.0674, M+H) showed a FI at *m/z* 299.0767 representing glucuronidation of one of the hydroxy groups at the methoxybenzyl moiety.

As already described for 2C-I [17], the two *N*-demethoxybenzyl-*O*-demethyl metabolites (**2** and **3**) were conjugated with an acetyl group forming two isomers of *N*-demethoxybenzyl-*O*-demethyl-*N*-acetyl-25I-NBOMe (**39** and **40**, PM at *m/z* 336.0091 M+H). In the following only isomer 1 (**39**) will be discussed. This conjugation reaction could be catalyzed by the *N*-acetyl-transferase (NAT) [30]. The fragmentation pattern was similar to that of the unacetylated

metabolites, but FI at *m/z* 209.1052 resulted from a loss of iodine as a radical and FI at *m/z* 336.0091 represented the *N*-acetylated 2C part with iodine.

O,O-bis-demethylation at the 2C part (**7**) led to hydroquinone, which could be conjugated with glutathione (GSH) by the glutathione-*S*-transferase [31]. The corresponding degradation products of GSH [31] [31] *O,O-bis*-demethyl-*S*-methyl (**41**, PM at *m/z* 446.0281, M+H) and the *O,O-bis*-demethyl-acetylcysteine (**51**, PM at *m/z* 561.0551, M+H) metabolites could be detected. Both spectra showed FIs of the unchanged methoxybenzyl moiety (*m/z* 91.0548 and 121.0653). Both metabolites showed fragmentation patterns for the postulated rearrangement reaction. The *S*-methyl metabolite (**41**) formed two FIs representing the rearranged *O,O-bis*-demethylated-*S*-methylated (*m/z* 322.9603) and *S*-demethylated (*m/z* 307.9368) 2C part. The spectrum of the acetylcysteine conjugated metabolite (**51**) showed one FI at *m/z* 432.0130 representing the *O,O-bis*-demethyl sulfide and one at *m/z* 455.0130 representing the rearranged 2C part conjugated with the intact *N*-acetylcysteine part.

Another conjugation formed three different metabolites. In the following only one metabolite will be discussed in detail due to similar fragmentation characteristics. The *bis*-hydroxylation at the methoxybenzyl moiety (**37** and **38**) could form a catechol structure (vicinal *bis*-hydroxylation). These metabolites could be a substrate for the catechol-*O*-methyl-transferase (COMT). Products of this conjugation could be found. In detail, the *bis*-hydroxy-*O*-methyl metabolite (**46**, PM at *m/z* 474.0772, M+H) showed the FI at *m/z* 167.0708 resulted from a shift of the FI at *m/z* 153.0552 by loss of one methyl group (+ 14.0156 u) representing the product of the COMT reaction. In addition, the FIs at *m/z* 290.9882 and 308.0148 represented the unchanged 2C part. The PM at *m/z* 474.0772 could not be found in the MS^2 spectra (marked with brackets in Fig. 3). The other two metabolites formed by the COMT were the *O,O-bis*-demethyl-*bis*-hydroxy-*O*-methyl metabolite (**42**, PM at 446.0459, M+H) and the *O*-demethyl-*bis*-hydroxy-*O*-methyl metabolite (**43**, PM at *m/z* 460.0616, M+H, Table. 2).

Proposed metabolic pathways

According to the metabolites identified in rat and human urine after cleavage of conjugates (Table 1), the following metabolic pathways, depicted in Fig. 4, could be proposed: mono-demethylation (**12, 13,** and **14**), *bis*-demethylation (**7**, **8,** and **9**), *tris*-demethylation (**6**) of the methoxy groups, mono- and *bis*-hydroxylation (**32-36; 38**), *N*-demethoxybenzylation (**5**), and combinations of mono-hydroxylation with mono-demethylation (**25-30**), and *bis*-demethylation (**15-21**) as well as *bis*-hydroxylation with mono-demethylation (**37**) and *N*-demethoxybenzylation with mono-demethylation (**2** and **3**) followed by oxidative deamination and oxidation to the corresponding carboxylic acid (**4**).

In summary, *O*-demethylation seemed to be the main metabolic pathway and *N*-demethoxybenzylation only a minor one in humans and rats. However, the relative abundance of the different metabolites varied between the species, but it should also be kept in mind that the rat urines were pooled over 24 h and the human urine was collected at an unknown time after administration of an unknown dose. Finally, the relation of the metabolites may vary over the time of excretion. A further limitation is that the rough estimation of relative abundances was based on the assumption that all compounds would show similar peak areas in the applied LC-MS system if present in the same concentration.

The following phase II metabolites could be proposed for humans and/or rats as given in Fig. 4 and in Table 2: glucuronidation (G) and/or sulfation (S) of the *O*-demethyl metabolites (**56G-58G,** and **50S**), of the *O,O-bis*-demethyl metabolites (**53G-55G** and **47S-49S**), of *O,O,O-tris*-demethyl metabolite (**52G, 44S**, and **45S**), of the *O*-demethyl-hydroxy metabolites (**63G-67G**), of the *O,O-bis*-demethyl-hydroxy metabolites (**59G-62G**), and of the hydroxy metabolites (**68G** and **69G**). Glutathione conjugation could be proposed for the *O,O-bis*-demethyl metabolite isomer 1 (**41GSH** and **51GSH**), *N*-acetylation for the *N*-demethoxybenzyl-*O*-demethyl metabolites (**39AC** and **40AC**), and *O*-methylation for the *bis*-hydroxy metabolite (**46ME**), the *O*-demethyl-*bis*-hydroxy metabolite (**43ME**), and the *O,O-bis*-demethyl-*bis*-hydroxy-*O*-methyl metabolite (**42ME**).

In summary, all phase II pathways could be proposed for both species with the exception of the *N*-acetylation, which was observed only in rats after the high dose. Again, the relative abundance also of the different conjugates varied between the species, but this was only a rough estimation as already discussed above.

CYP Initial Screening

For identification of the CPYs catalyzing the initial metabolic steps, the ten most abundant human hepatic CYPs were incubated under conditions allowing a statement on the general involvement of a particular CYP enzyme. As summarized in Table 3, CYP2C9 and CYP2C19 were mainly involved in *O*-demethylation, CYP1A2 and CYP3A4 in hydroxylation, and CYP3A4 in *N*-demethoxybenzylation. However, not all isomers detected in urine could be found in these incubations, e.g. only one metabolite *O*-demethylated at the 2C part.

Toxicological detection of 25I-NBOMe by GC-MS SUSA

Unfortunately, 25I-NBOMe and/or its metabolites could not be detected in rat urine after a common single dose reported in trip reports (https://www.erowid.org) and scaled by dose-by-factor approach from man to rat according to Sharma and McNeill [32]. The authentic human urine sample was also negative. This could be caused by lower sensitivity of GC-MS and most probably by the sample preparation. Preliminary studies showed that the NBOMe's degraded in part during hydrolysis and exposure to oxygen. Only after the high dose, enzymatic cleavage of conjugates, solid-phase extraction, and acetylation according to Welter et al. [25], small amounts of 25I-NBOMe *O*-demethyl metabolites could be detected.

Toxicological detection of 25I-NBOMe by LC-MS^n SUSA

The LC-MS^n approach was able to detect 25I-NBOMe and/or its metabolites in rat urine after the 0.05 or 0.1 mg/kg BW dose as well as in the authentic human urine sample. A list of the detected metabolites is given in Table 4. As already mentioned above, the differences of detected analytes in the human and rat urine samples could be caused by different doses and urine collection times.

Toxicological detection of 25I-NBOMe by LC-HR-MS/MS SUSA

In addition, the detectability was also tested by the new LC-HR-MS/MS screening approach (Helfer et al., submitted). As expected, this approach was also able to detect 25I-NBOMe and/or its metabolites in rat urine after the 0.05 or 0.1 mg/kg BW dose as well as in the authentic human urine sample. A list of the identified or detected metabolites in human as well as in rat samples is given in Table 5. Again, the differences of detected analytes in the human and rat urine samples could be caused by different doses and urine collection times. Figure 5 shows reconstituted ion chromatograms of the human urine sample indicating various metabolites, which could be identified according to definition given above. In this sample, the parent drug could only be detected in contrast to the rat urine samples after the 0.1 mg/kg BW dose.

Conclusion

25I-NBOMe was extensively metabolized with *O*-demethylation, *O,O-bis*-demethylation, and hydroxylations as predominant pathways. Several CYP isoenzymes were involved in formation of the main metabolites. An intake could be detected mainly via its metabolites by low and high resolution LC-MS SUSAs.

Acknowledgements

The authors like to thank Julia Dinger, Lilian H. J. Richter, Carsten Schröder, Gabriele Ulrich, Lea Wagmann, Armin A. Weber, Jessica Welter, and Carina S. D. Wink for support and/or helpful discussion.

References

1. Maurer HH (2010) Chemistry, Pharmacology, and Metabolism of Emerging Drugs of Abuse [review]. Ther Drug Monit 32:544-549
2. Hansen M, Phonekeo K, Paine JS, Leth-Petersen S, Begtrup M, Brauner-Osborne H, Kristensen JL (2014) Synthesis and structure-activity relationships of N-benzyl phenethylamines as 5-HT2A/2C agonists. ACS Chem Neurosci 5:243-249
3. Braden MR, Parrish JC, Naylor JC, Nichols DE (2006) Molecular interaction of serotonin 5-HT2A receptor residues Phe339(6.51) and Phe340(6.52) with superpotent N-benzyl phenethylamine agonists. Mol Pharmacol 70:1956-1964
4. Poklis JL, Nanco CR, Troendle MM, Wolf CE, Poklis A (2014) Determination of 4-bromo-2,5-dimethoxy-N-[(2-methoxyphenyl)methyl]-benzeneethanamine (25B-NBOMe) in serum and urine by high performance liquid chromatography with tandem mass spectrometry in a case of severe intoxication. Drug Test Anal 6:764-769
5. Poklis JL, Devers KG, Arbefeville EF, Pearson JM, Houston E, Poklis A (2014) Postmortem detection of 25I-NBOMe [2-(4-iodo-2,5-dimethoxyphenyl)-N-[(2-methoxyphenyl)methyl]ethanamine] in fluids and tissues determined by high performance liquid chromatography with tandem mass spectrometry from a traumatic death. Forensic Sci Int 234:e14-e20
6. Rose SR, Poklis JL, Poklis A (2013) A case of 25I-NBOMe (25-I) intoxication: a new potent 5-HT2A agonist designer drug. Clin Toxicol (Phila) 51:174-177
7. Stellpflug SJ, Kealey SE, Hegarty CB, Janis GC (2014) 2-(4-Iodo-2,5-dimethoxyphenyl)-N-[(2-methoxyphenyl)methyl]ethanamine (25I-NBOMe): clinical case with unique confirmatory testing. J Med Toxicol 10:45-50
8. Walterscheid JP, Phillips GT, Lopez AE, Gonsoulin ML, Chen HH, Sanchez LA (2014) Pathological findings in 2 cases of fatal 25I-NBOMe toxicity. Am J Forensic Med Pathol 35:20-25

9. Tang MH, Ching CK, Tsui MS, Chu FK, Mak TW (2014) Two cases of severe intoxication associated with analytically confirmed use of the novel psychoactive substances 25B-NBOMe and 25C-NBOMe. Clin Toxicol (Phila) 52:561-565
10. Poklis JL, Charles J, Wolf CE, Poklis A (2013) High-performance liquid chromatography tandem mass spectrometry method for the determination of 2CC-NBOMe and 25I-NBOMe in human serum. Biomed Chromatogr 27:1794-1800
11. Maurer HH (2010) Analytical toxicology [review]. Experientia 100:317-337
12. Maurer HH (2012) How Can Analytical Diagnostics in Clinical Toxicology Be Successfully Performed Today? Ther Drug Monit 34:561-564
13. Maurer HH (2013) What is the future of (ultra)high performance liquid chromatography coupled to low and high resolution mass spectrometry for toxicological drug screening? [review]. J Chromatogr A 1292:19-24
14. Wink CSD, Meyer MR, Braun T, Turcant A, Maurer HH (2015) Biotransformation and detectability of the designer drug 2,5-dimethoxy-4-propylphenethylamine (2C-P) studied in urine by GC-MS, LC-MS^n and LC-high resolution-MS^n. Anal Bioanal Chem 407:831-843
15. Theobald DS, Fritschi G, Maurer HH (2007) Studies on the toxicological detection of the designer drug 4-bromo-2,5-dimethoxy-beta-phenethylamine (2C-B) in rat urine using gas chromatography-mass spectrometry. J Chromatogr B 846:374-377
16. Theobald DS, Maurer HH (2007) Identification of monoamine oxidase and cytochrome P450 isoenzymes involved in the deamination of phenethylamine-derived designer drugs (2C-series). Biochem Pharmacol 73:287-297
17. Theobald DS, Putz M, Schneider E, Maurer HH (2006) New designer drug 4-iodo-2,5-dimethoxy-beta-phenethylamine (2C-I): studies on its metabolism and toxicological detection in rat urine using gas chromatographic/mass spectrometric and capillary electrophoretic/mass spectrometric techniques. J Mass Spectrom 41:872-886

18. Theobald DS, Maurer HH (2006) Studies on the metabolism and toxicological detection of the designer drug 4-ethyl-2,5-dimethoxy-beta-phenethylamine (2C-E) in rat urine using gas chromatographic-mass spectrometric techniques. J Chromatogr B 842:76-90

19. Theobald DS, Maurer HH (2006) Studies on the metabolism and toxicological detection of the designer drug 2,5-dimethoxy-4-methyl-beta-phenethylamine (2C-D) in rat urine using gas chromatographic-mass spectrometric techniques. J Mass Spectrom 41:1509-1519

20. Theobald DS, Staack RF, Puetz M, Maurer HH (2005) New designer drug 2,5-dimethoxy-4-ethylthio-beta-phenethylamine (2C-T-2): studies on its metabolism and toxicological detection in rat urine using gas chromatography/mass spectrometry. J Mass Spectrom 40:1157-1172

21. Theobald DS, Fehn S, Maurer HH (2005) New designer drug 2,5-dimethoxy-4-propylthiophenethylamine (2C-T-7): studies on its metabolism and toxicological detection in rat urine using gas chromatography/mass spectrometry. J Mass Spectrom 40:105-116

22. Meyer MR, Lindauer C, Welter J, Maurer HH (2014) Dimethocaine, a synthetic cocaine derivative: Studies on its in vivo metabolism and its detectability in urine by LC-HR-MS^n and GC-MS using a rat model. Anal Bioanal Chem 406:1845-1854

23. Wissenbach DK, Meyer MR, Remane D, Philipp AA, Weber AA, Maurer HH (2011) Drugs of abuse screening in urine as part of a metabolite-based LC-MS(n) screening concept. Anal Bioanal Chem 400:3481-3489

24. Welter J, Kavanagh P, Meyer MR, Maurer HH (2015) Benzofuran analogues of amphetamine and methamphetamine: Studies on the metabolism and toxicological analysis of 5-APB and 5-MAPB in urine and plasma using GC-MS and LC-(HR)-MS^n techniques. Anal Bioanal Chem 407:1371-1388

25. Welter J, Meyer MR, Wolf E, Weinmann W, Kavanagh P, Maurer HH (2013) 2-Methiopropamine, a thiophene analogue of methamphetamine: Studies on its metabolism and detectability in the rat and human using GC-MS and LC-(HR)-MS techniques. Anal Bioanal Chem 405:3125-3135

26. Helfer AG, Turcant A, Boels D, Ferec S, Lelievre B, Welter J, Meyer MR, Maurer HH (2015) Elucidation of the metabolites of the novel psychoactive substance 4-methyl-*N*-ethyl-cathinone (4-MEC) in human urine and pooled liver microsomes by GC-MS and LC-HR-MS/MS techniques and of its detectability by GC-MS or LC-MS^n standard screening approaches. Drug Test Anal, DOI 10.1002/dta.1682

27. Wissenbach DK, Meyer MR, Remane D, Weber AA, Maurer HH (2011) Development of the first metabolite-based LC-MSn urine drug screening procedure - exemplified for antidepressants. Anal Bioanal Chem 400:79-88

28. Maurer HH, Wissenbach DK, Weber AA (2014) Maurer/Wissenbach/Weber MWW LC-MSn Library of Drugs, Poisons, and their Metabolites. Wiley-VCH, Weinheim

29. Broecker S, Herre S, Wust B, Zweigenbaum J, Pragst F (2011) Development and practical application of a library of CID accurate mass spectra of more than 2,500 toxic compounds for systematic toxicological analysis by LC-QTOF-MS with data-dependent acquisition. Anal Bioanal Chem 400:101-117

30. Meyer MR, Robert A, Maurer HH (2014) Toxicokinetics of novel psychoactive substances: Characterization of N-acetyltransferase (NAT) isoenzymes involved in the phase II metabolism of 2C designer drugs. Toxicol Lett 227:124-128

31. Meyer MR, Richter LHR, Maurer HH (2014) Methylenedioxy designer drugs: Mass spectrometric characterization of their glutathione conjugates by means of liquid chromatography-high-resolution mass spectrometry/mass spectrometry and studies on their glutathionyl transferase inhibition potency. Anal Chim Acta 822:37-50

32. Sharma V, McNeill JH (2009) To scale or not to scale: the principles of dose extrapolation. Br J Pharmacol 157:907-921

Table 1 List of 25I-NBOMe and its phase I metabolites detected in human (H) or rat (R) urine together with the masses of their precursor mass (PM) recorded in MS^1, the corresponding characteristic fragment ions (FI) in MS^2, the calculated exact masses, the corresponding elemental composition, the deviation of the measured from the calculated masses, given as errors in ppm, and the retention times (RT) in min. The metabolites were sorted by mass and RT.

No.	Metabolites and characteristic ions Measured accurate masses, u	Relative intensity in MS^2, %	Calculated exact masses, *m/z*	Elemental composition	Error, ppm	RT, min
1	**25I-NBOMe (H/R)**					9.21
	MS^1 PM at *m/z* 428.0720 (M+H)	13	428.0717	$C_{18}H_{23}O_3NI$	0.65	
	MS^2 FI at *m/z* 91.0547	48	91.0548	C_7H_7	-0.82	
	FI at *m/z* 121.0650	100	121.0653	C_8H_9O	-2.81	
	FI at *m/z* 272.1408	3	272.1412	$C_{17}H_{20}O_3$	-1.64	
	FI at *m/z* 290.9878	1	290.9882	$C_{10}H_{12}O_2I$	-1.40	
	FI at *m/z* 305.9996	0.5	305.9991	$C_{10}H_{13}O_2NI$	1.61	
2	**25I-NBOMe-M (*N*-demethoxybenzyl-*O*-demethyl-) isomer 1 (H/R)**					4.89
	MS^1 PM at *m/z* 293.9983 (M+H)	4	293.9991	$C_9H_{13}O_2NI$	-2.74	
	MS^2 FI at *m/z* 135.0440	61	135.0446	$C_8H_7O_2$	-4.48	
	FI at *m/z* 150.0674	56	150.0681	$C_9H_{10}O_2$	-4.53	
	FI at *m/z* 261.9486	27	261.9491	$C_8H_7O_2I$	-1.84	
	FI at *m/z*276.9716	100	276.9726	$C_9H_{10}O_2I$	-3.46	
3	**25I-NBOMe-M (*N*-demethoxybenzyl-*O*-demethyl-) isomer 2 (H/R)**					4.98
	MS^1 PM at *m/z* 293.9983 (M+H)	6	293.9991	$C_9H_{13}O_2NI$	-2.74	
	MS^2 FI at *m/z* 135.0441	29	135.0446	$C_8H_7O_2$	-3.74	
	FI at *m/z* 150.0676	31	150.0681	$C_9H_{10}O_2$	-3.20	
	FI at *m/z* 261.9486	71	261.9491	$C_8H_7O_2I$	-1.84	
	FI at *m/z* 276.9719	100	276.9726	$C_9H_{10}O_2I$	-2.37	
4	**25I-NBOMe-M (*N*-demethoxybenzyl-*O*-demethyl-deamino-HOOC-) (H/R)**					7.24
	MS^1 PM at *m/z* 306.9467 (M-H)	3	306.9467	$C_9H_8O_4I$	0	
	MS^2 FI at *m/z* 126.9039	100	126.9045	I	-4.55	
	FI at *m/z* 247.9337	14	247.9334	$C_7H_5O_2I$	1.08	
	FI at *m/z* 262.9574	6	262.9569	$C_8H_8O_2I$	1.87	
5	**25I-NBOMe-M (*N*-demethoxybenzyl-) (H/R)**					6.36
	MS^1 PM at *m/z* 308.0147 (M+H)	4	308.0148	$C_{10}H_{15}O_2NI$	-0.18	
	MS^2 FI at *m/z* 149.0597	22	149.0603	$C_9H_9O_2$	-3.72	
	FI at *m/z* 260.9404	36	260.9413	$C_8H_6O_2I$	-3.28	
	FI at *m/z* 275.9639	88	275.9647	$C_9H_9O_2I$	-3.01	
	FI at *m/z* 290.9872	100	290.9882	$C_{10}H_{12}O_2I$	-3.46	
6	**25I-NBOMe-M (*O,O,O-tris*-demethyl-) (H/R)**					5.76
	MS^1 PM at *m/z* 386.0243 (M+H)	15	386.0248	$C_{15}H_{17}O_3NI$	-1.22	
	MS^2 FI at *m/z* 107.0494	100	107.0497	C_7H_7O	-2.71	
	FI at *m/z* 136.0519	36	136.0524	$C_8H_8O_2$	-3.90	
	FI at *m/z* 262.9563	77	262.9569	$C_8H_8O_2I$	-2.31	
	FI at *m/z* 279.9827	36	279.9835	$C_8H_{11}O_2NI$	-2.70	
7	**25I-NBOMe-M (*O,O-bis*-demethyl-) isomer1 (H/R)**					6.61
	MS^1 PM at *m/z* 400.0405 (M+H)	8	400.0404	$C_{16}H_{19}O_3NI$	0.19	
	MS^2 FI at *m/z* 91.0547	44	91.0548	C_7H_7	-0.82	
	FI at *m/z* 121.0649	100	121.0653	C_8H_9O	-3.63	
	FI at *m/z* 256.1098	1	256.1099	$C_{16}C_{16}O_3$	-0.57	
	FI at *m/z* 274.9562	1	274.9569	$C_9H_8O_2I$	-2.57	
8	**25I-NBOMe-M (*O,O-bis*-demethyl-) isomer 2 (H/R)**					7.37

	MS^1	PM at *m/z* 400.0400 (M+H)	13	400.0404	$C_{16}H_{19}O_3NI$	-1.06	
	MS^2	FI at *m/z* 107.0495	100	107.0497	C_7H_7O	-1.77	
		FI at *m/z* 261.9487	13	261.9491	$C_8H_7O_2I$	-1.46	
		FI at *m/z* 276.9718	80	276.9726	$C_9H_{10}O_2I$	-2.73	
		FI at *m/z* 293.9984	30	293.9991	$C_9H_{13}O_2NI$	-2.40	
9	**25I-NBOMe-M (*O,O-bis*-demethyl-) isomer 3 (H/R)**						7.51
	MS^1	PM at *m/z* 400.0405 (M+H)	17	400.0404	$C_{16}H_{19}O_3NI$	0.19	
	MS^2	FI at *m/z* 107.0495	100	107.0497	C_7H_7O	-1.77	
		FI at *m/z* 261.9487	29	261.9491	$C_8H_7O_2I$	-1.46	
		FI at *m/z* 276.9718	83	276.9726	$C_9H_{10}O_2I$	-2.73	
		FI at *m/z* 293.9983	33	293.9991	$C_9H_{13}O_2NI$	-2.74	
10	**25I-NBOMe-M (*O*-demethyl-dehydro-) isomer1 (H/R)**						7.19
	MS^1	PM at *m/z* 412.0402 (M+H)	33	412.0404	$C_{17}H_{19}O_3NI$	-0.54	
	MS^2	FI at *m/z* 107.0494	100	107.0497	C_7H_7O	-2.71	
		FI at *m/z* 179.0939	13	179.0946	$C_{10}H_{13}O_2N$	-4.07	
		FI at *m/z* 276.9715	15	276.9726	$C_9H_{10}O_2I$	-3.82	
		FI at *m/z* 305.9979	66	305.9991	$C_{10}H_{13}O_2NI$	-3.94	
11	**25I-NBOMe-M (*O*-demethyl-dehydro-) isomer2 (H/R)**						7.83
	MS^1	PM at *m/z* 412.0401 (M+H)	5	412.0404	$C_{17}H_{19}O_3NI$	-0.78	
	MS^2	FI at *m/z* 91.0547	46	91.0548	C_7H_7	-0.82	
		FI at *m/z* 121.0650	100	121.0653	C_8H_9O	-2.81	
		FI at *m/z* 285.1356	16	285.1365	$C_{17}H_{19}O_3N$	-3.14	
		FI at *m/z* 290.9748	19	290.9756	$C_9H_{10}O_2NI$	-2.86	
12	**25I-NBOMe-M (*O*-demethyl-) isomer 1 (H/R)**						8.08
	MS^1	PM at *m/z* 414.0552 (M+H)	6	414.0561	$C_{17}H_{21}O_3NI$	-2.11	
	MS^2	FI at *m/z* 91.0546	48	91.0548	C_7H_7	-1.92	
		FI at *m/z* 121.0649	100	121.0653	C_8H_9O	-3.63	
		FI at *m/z* 270.1252	2	270.1256	$C_{17}H_{18}O_3$	-1.46	
		FI at *m/z* 287.1509	1	287.1521	$C_{17}H_{21}O_3N$	-4.33	
		FI at *m/z* 397.0288	1	397.0301	$C_{17}H_{18}O_3I$	-3.20	
13	**25I-NBOMe-M (*O*-demethyl-) isomer 2 (H/R)**						8.25
	MS^1	PM at *m/z* 414.0561 (M+H)	10	414.0561	$C_{17}H_{21}O_3NI$	0	
	MS^2	FI at *m/z* 91.0547	50	91.0548	C_7H_7	-0.82	
		FI at *m/z* 121.0650	100	121.0653	C_8H_9O	-2.81	
		FI at *m/z* 258.1256	1	258.1256	$C_{16}H_{18}O_3$	0	
		FI at *m/z* 270.1259	0.4	270.1256	$C_{17}H_{18}O_3N$	1.13	
14	**25I-NBOMe-M (*O*-demethyl-) isomer 3 (H/R)**						8.51
	MS^1	PM at *m/z* 414.0561 (M+H)	10	414.0561	$C_{17}H_{21}O_3NI$	0	
	MS^2	FI at *m/z* 107.0494	100	107.0497	C_7H_7O	-2.71	
		FI at *m/z* 275.9639	44	275.9647	$C_9H_9O_2I$	-3.01	
		FI at *m/z* 290.9872	79	290.9882	$C_{10}H_{12}O_2I$	-3.46	
		FI at *m/z* 308.0136	30	308.0148	$C_{10}H_{15}O_2NI$	-3.75	
15	**25I-NBOMe-M (*O,O-bis*-demethyl-HO-) isomer 1 (H/R)**						5.77
	MS^1	PM at *m/z* 416.0355 (M+H)	8	416.0353	$C_{16}H_{19}O_4NI$	0.39	
	MS^2	FI at *m/z* 107.0495	38	107.0497	C_7H_7O	-1.77	
		FI at *m/z* 137.0598	100	137.0603	$C_8H_9O_2I$	-3.32	
		FI at *m/z* 272.1039	1	272.1049	$C_{16}H_{16}O_4$	-3.53	
		FI at *m/z* 399.0078	1	399.0093	$C_{16}H_{16}O_4I$	-3.85	
16	**25I-NBOMe-M (*O,O-bis*-demethyl-HO-) isomer 2 (H/R)**						6.24
	MS^1	PM at *m/z* 416.0355 (M+H)	12	416.0353	$C_{16}H_{19}O_4NI$	0.39	
	MS^2	FI at *m/z* 123.0443	100	123.0446	$C_7H_7O_2$	-2.48	
		FI at *m/z* 150.0677	31	150.0681	$C_9H_{10}O_2$	-2.53	
		FI at *m/z* 276.9720	90	276.9726	$C_9H_{10}O_2I$	-2.01	
		FI at *m/z* 293.9984	32	293.9991	$C_9H_{13}O_2NI$	-2.40	
17	**25I-NBOMe-M (*O,O-bis*-demethyl-HO-) isomer 3 (H/R)**						6.31

	MS^1	PM at *m/z* 416.0355 (M+H)	15	416.0353	$C_{16}H_{19}O_4NI$	0.39	
	MS^2	FI at *m/z* 123.0442	100	123.0446	$C_7H_7O_2$	-3.29	
		FI at *m/z* 150.0677	29	150.0681	$C_9H_{10}O_2$	-2.53	
		FI at *m/z* 276.9717	94	276.9726	$C_9H_{10}O_2I$	-2.01	
		FI at *m/z* 293.9984	32	293.9991	$C_9H_{13}O_2NI$	-2.40	
18	**25I-NBOMe-M (*O,O-bis*-demethyl-HO-) isomer 4 (H)**						6.50
	MS^1	PM at *m/z* 416.0355 (M+H)	15	416.0353	$C_{16}H_{19}O_4NI$	0.39	
	MS^2	FI at *m/z* 107.0496	100	107.0497	C_7H_7O	-0.84	
		FI at *m/z* 277.9436	66	277.9440	$C_8H_7O_3I$	-1.43	
		FI at *m/z* 292.9670	75	292.9675	$C_9H_{10}O_3I$	-1.61	
		FI at *m/z* 309.9932	33	309.9940	$C_9H_{13}O_3NI$	-2.65	
19	**25I-NBOMe-M (*O,O-bis*-demethyl-HO-) isomer 5 (H/R)**						6.78
	MS^1	PM at *m/z* 416.0351 (M+H)	17	416.0353	$C_{16}H_{19}O_4NI$	-0.57	
	MS^2	FI at *m/z* 123.0442	100	123.0446	$C_7H_7O_2$	-3.29	
		FI at *m/z* 150.0675	19	150.0681	$C_9H_{10}O_2$	-3.86	
		FI at *m/z* 276.9716	66	276.9726	$C_9H_{10}O_2I$	-3.46	
		FI at *m/z* 293.9984	24	293.9991	$C_9H_{13}O_2NI$	-2.40	
20	**25I-NBOMe-M (*O,O-bis*-demethyl-HO-) isomer 6 (H/R)**						6.94
	MS^1	PM at *m/z* 416.0350 (M+H)	20	416.0353	$C_{16}H_{19}O_4NI$	-0.81	
	MS^2	FI at *m/z* 123.0441	100	123.0446	$C_7H_7O_2$	-4.10	
		FI at *m/z* 150.0674	13	150.0681	$C_9H_{10}O_2$	-4.53	
		FI at *m/z* 276.9717	71	276.9726	$C_9H_{10}O_2I$	-3.09	
		FI at *m/z* 293.9983	24	293.9991	$C_9H_{13}O_2NI$	-2.74	
21	**25I-NBOMe-M (*O,O-bis*-demethyl-HO-) isomer 7 (R)**						7.26
	MS^1	PM at *m/z* 416.0325 (M+H)	11	416.0353	$C_{16}H_{19}O_4NI$	-6.82	
	MS^2	FI at *m/z* 107.0495	90	107.0497	C_7H_7O	-1.77	
		FI at *m/z* 165.0785	52	165.0790	$C_9H_{11}O_2N$	-2.90	
		FI at *m/z* 291.9827	100	291.9835	$C_9H_{11}O_2NI$	-2.59	
		FI at *m/z* 398.0244	14	398.0253	$C_{16}H_{17}O_3NI$	-2.31	
22	**25I-NBOMe-M (dehydro-) (H/R)**						7.89
	MS^1	PM at *m/z* 426.0559 (M+H)	25	426.0561	$C_{18}H_{21}O_3NI$	-0.41	
	MS^2	FI at *m/z* 91.0547	47	91.0548	C_7H_7	-0.82	
		FI at *m/z* 121.0650	100	121.0653	C_8H_9O	-2.81	
		FI at *m/z* 287.9514	1	287.9522	$C_9H_7O_2NI$	-2.63	
		FI at *m/z* 303.9824	8	303.9835	$C_{10}H_{11}O_2NI$	-3.47	
23	**25I-NBOMe-M (*O*-demethyl-dehydro-HO-) isomer 1 (H/R)**						6.07
	MS^1	PM at *m/z* 428.0348 (M+H)	30	428.0353	$C_{17}H_{19}O_4NI$	-1.26	
	MS^2	FI at *m/z* 123.0442	100	123.0446	$C_7H_7O_2$	-3.29	
		FI at *m/z* 179.0940	14	179.0946	$C_{10}H_{13}O_2N$	-3.51	
		FI at *m/z* 276.9715	18	276.9726	$C_9H_{10}O_2I$	-3.82	
		FI at *m/z* 305.9984	83	305.9991	$C_{10}H_{13}O_2NI$	-2.31	
24	**25I-NBOMe-M (*O*-demethyl-dehydro-HO-) isomer 2 (R)**						6.26
	MS^1	PM at *m/z* 428.0348 (M+H)	33	428.0353	$C_{17}H_{19}O_4NI$	-1.26	
	MS^2	FI at *m/z* 107.0494	100	107.0497	C_7H_7O	-2.71	
		FI at *m/z* 178.0625	23	178.0630	$C_{10}H_{10}O_3$	-2.78	
		FI at *m/z* 292.9666	8	292.9675	$C_9H_{10}O_3I$	-2.98	
		FI at *m/z* 321.9927	54	321.9940	$C_{10}H_{13}O_3NI$	-4.10	
25	**25I-NBOMe-M (*O*-demethyl-HO-) isomer 1 (H)**						7.15
	MS^1	PM at *m/z* 430.0515 (M+H)	12	430.0510	$C_{17}H_{21}O_4NI$	1.19	
	MS^2	FI at *m/z* 109.0651	100	109.0653	C_7H_9O	-2.20	
		FI at *m/z* 137.0598	67	137.0603	$C_8H_9O_2$	-3.32	
		FI at *m/z* 276.9716	18	276.9726	$C_9H_{10}O_2I$	-3.46	
		FI at *m/z* 293.9983	7	293.9991	$C_9H_{13}O_2NI$	-2.74	
26	**25I-NBOMe-M (*O*-demethyl-HO-) isomer 2 (H/R)**						7.24
	MS^1	PM at *m/z* 430.0515 (M+H)	6	430.0510	$C_{17}H_{21}O_4NI$	1.19	
	MS^2	FI at *m/z* 107.0495	44	107.0497	C_7H_7O	-1.77	
		FI at *m/z* 137.0598	100	137.0603	$C_8H_9O_2$	-3.32	

		FI at *m/z* 286.1198	2	286.1205	$C_{17}H_{18}O_4$	-2.48	
		FI at *m/z* 303.1472	1	303.1471	$C_{17}H_{21}O_4N$	0.47	
27	**25I-NBOMe-M (*O*-demethyl-HO-) isomer 3 (H/R)**						7.35
	MS^1	PM at *m/z* 430.0511 (M+H)	11	430.0510	$C_{17}H_{21}O_4NI$	0.26	
	MS^2	FI at *m/z* 107.0495	40	107.0497	C_7H_7O	-1.77	
		FI at *m/z* 137.0598	100	137.0603	$C_8H_9O_2$	-3.32	
		FI at *m/z* 276.9726	1	276.9726	$C_9H_{10}O_2I$	0	
		FI at *m/z* 286.1212	1	286.1205	$C_{17}H_{18}O_4$	2.41	
28	**25I-NBOMe-M (*O*-demethyl-HO-) isomer 4 (H)**						7.36
	MS^1	PM at *m/z* 430.0511 (M+H)	13	430.0510	$C_{17}H_{21}O_4NI$	0.26	
	MS^2	FI at *m/z* 123.0442	100	123.0446	$C_7H_7O_2$	-3.29	
		FI at *m/z* 275.9641	49	275.9647	$C_9H_9O_2I$	-2.29	
		FI at *m/z* 290.9874	95	290.9882	$C_{10}H_{12}O_2I$	-2.77	
		FI at *m/z* 308.0137	32	308.0148	$C_{10}H_{15}O_2NI$	-3.43	
29	**25I-NBOMe-M (*O*-demethyl-HO-) isomer 5 (H)**						7.92
	MS^1	PM at *m/z* 430.0509 (M+H)	8	430.0510	$C_{17}H_{21}O_4NI$	-0.20	
	MS^2	FI at *m/z* 123.0442	100	123.0446	$C_7H_7O_2$	-3.29	
		FI at *m/z* 275.9641	40	275.9647	$C_9H_9O_2I$	-2.29	
		FI at *m/z* 290.9873	70	290.9882	$C_{10}H_{12}O_2I$	-3.12	
		FI at *m/z* 308.0137	21	308.0148	$C_{10}H_{15}O_2NI$	-3.43	
30	**25I-NBOMe-M (*O*-demethyl-HO-) isomer 6 (H)**						7.95
	MS^1	PM at *m/z* 430.0509 (M+H)	6	430.0510	$C_{17}H_{21}O_4NI$	-0.20	
	MS^2	FI at *m/z* 91.0547	47	91.0548	C_7H_7	-0.82	
		FI at *m/z* 121.0650	100	121.0653	C_8H_9O	-2.81	
		FI at *m/z* 291.9825	3	291.9835	$C_9H_{11}O_2NI$	-3.27	
		FI at *m/z* 412.0403	8	412.0410	$C_{17}H_{19}O_3NI$	-1.63	
31	**25I-NBOMe-M (dehydro-HO-) (H/R)**						7.09
	MS^1	PM at *m/z* 442.0507 (M+H)	21	442.0510	$C_{18}H_{21}O_4NI$	-0.65	
	MS^2	FI at *m/z* 91.0547	53	91.0548	C_7H_7	-0.82	
		FI at *m/z* 121.0650	100	121.0653	C_8H_9O	-2.81	
		FI at *m/z* 304.9539	2	304.9549	$C_9H_8O_3NI$	-3.27	
		FI at *m/z* 319.9775	6	319.9784	$C_{10}H_{11}O_3NI$	-2.72	
32	**25I-NBOMe-M (HO-) isomer 1 (R)**						7.72
	MS^1	PM at *m/z* 444.0668 (M+H)	16	444.0666	$C_{18}H_{23}O_4NI$	0.37	
	MS^2	FI at *m/z* 91.0547	51	91.0548	C_7H_7	-0.82	
		FI at *m/z* 121.0650	100	121.0653	C_8H_9O	-2.81	
		FI at *m/z* 276.9361	2	276.9362	$C_8H_6O_3I$	-0.26	
		FI at *m/z* 306.9822	7	306.9831	$C_{10}H_{12}O_3I$	-3.00	
33	**25I-NBOMe-M (HO-) isomer 2 (H)**						8.24
	MS^1	PM at *m/z* 444.0668 (M+H)	16	444.0666	$C_{18}H_{23}O_4NI$	0.37	
	MS^2	FI at *m/z* 109.0651	100	109.0653	C_7H_9O	-2.20	
		FI at *m/z* 137.0597	78	137.0603	$C_8H_9O_2$	-4.05	
		FI at *m/z* 290.9872	32	290.9882	$C_{10}H_{12}O_2I$	-3.46	
		FI at *m/z* 308.0135	12	308.0148	$C_{10}H_{15}O_2NI$	-4.08	
34	**25I-NBOMe-M (HO-) isomer 3 (H/R)**						8.34
	MS^1	PM at *m/z*444.0667 (M+H)	9	444.0666	$C_{18}H_{23}O_4NI$	0.14	
	MS^2	FI at *m/z* 107.0494	43	107.0497	C_7H_7O	-2.71	
		FI at *m/z* 137.0598	100	137.0603	$C_8H_9O_2$	-3.32	
		FI at *m/z* 288.1353	2	288.1362	$C_{17}H_{20}O_4$	-2.98	
		FI at *m/z* 290.9872	1	290.9882	$C_{10}H_{12}O_2I$	-3.46	
35	**25I-NBOMe-M (HO-) isomer 4 (H)**						8.81
	MS^1	PM at *m/z* 444.0675 (M+H)	10	444.0666	$C_{18}H_{23}O_4NI$	1.94	
	MS^2	FI at *m/z* 91.0547	53	91.0548	C_7H_7	-0.82	
		FI at *m/z* 121.0651	100	121.0653	C_8H_9O	-1.98	
		FI at *m/z* 291.1589	4	291.1596	$C_{17}H_{23}O_4$	-2.52	
		FI at *m/z* 426.0553	3	426.0561	$C_{18}H_{21}O_3NI$	-1.81	

36	**25I-NBOMe-M (HO-) isomer 5 (H)**						8.91
	MS^1	PM at *m/z* 444.0650 (M+H)	7	444.0666	$C_{18}H_{23}O_4NI$	-3.69	
	MS^2	FI at *m/z* 137.0598	100	137.0603	$C_8H_9O_2$	-3.32	
		FI at *m/z* 275.9641	39	275.9647	$C_9H_9O_2I$	-2.29	
		FI at *m/z* 290.9873	83	290.9882	$C_{10}H_{12}O_2I$	-3.12	
		FI at *m/z* 308.0139	41	308.0148	$C_{10}H_{15}O_2NI$	-2.78	
37	**25I-NBOMe-M (*O*-demethyl-*bis*-HO-) (H/R)**						6.79
	MS^1	PM at *m/z* 446.0464 (M+H)	1	446.0459	$C_{17}H_{21}O_5NI$	1.12	
	MS^2	FI at *m/z* 153.0545	100	153.0552	$C_8H_9O_3$	-4.38	
		FI at *m/z* 261.9484	27	261.9491	$C_8H_7O_2I$	-2.60	
		FI at *m/z* 276.9717	95	276.9726	$C_9H_{10}O_2I$	-3.09	
		FI at *m/z* 293.9982	35	293.9991	$C_9H_{13}O_2NI$	-3.08	
38	**25I-NBOMe-M (*bis*-HO-) (H)**						7.39
	MS^1	PM at *m/z* 460.0616 (M+H)	1	460.0616	$C_{18}H_{23}O_5NI$	0	
	MS^2	FI at *m/z* 153.0550	88	153.0552	$C_8H_9O_3$	-1.11	
		FI at *m/z* 290.9885	100	290.9882	$C_{10}H_{12}O_2I$	1.01	
		FI at *m/z* 308.0142	37	308.0148	$C_{10}H_{15}O_2NI$	-1.81	
		FI at *m/z* 442.0516	8	442.0515	$C_{18}H_{21}O_4NI$	0.14	

Table 2 List of all phase II metabolites detected in human (H) or rat (R) urine together with the masses of their precursor mass (PM) recorded in MS^1, the corresponding characteristic fragment ions (FI) in MS^2, the calculated exact masses, the corresponding elemental composition, the deviation of the measured from the calculated masses, given as errors in ppm, and the retention times (RT) in min. The metabolites were sorted by mass and RT.

No.	Metabolites and characteristic ions Measured accurate masses, u		Relative intensity in MS^2, %	Calculated exact masses, u	Elemental composition	Error, ppm	RT, min
39	**25I-NBOMe-M (*N*-demethoxybenzyl-*O*-demethyl-) *N*-acetyl isomer 1 (R)**						7.43
	MS^1	PM at *m/z* 336.0075 (M+H)	16	336.0091	$C_{11}H_{15}O_3NI$	-4.83
	MS^2	FI at *m/z* 150.0678	88	150.0681	$C_9H_{10}O_2$	-1.87
		FI at *m/z* 209.1049	27	209.1052	$C_{11}H_{15}O_3N$	-1.41
		FI at *m/z* 261.9489	20	261.9491	$C_8H_7O_2I$	-0.69
		FI at *m/z* 276.9724	100	276.9726	$C_9H_{10}O_2I$	-0.57
		FI at *m/z* 293.9987	20	293.9991	$C_9H_{13}O_2NI$	-1.38
40	**25I-NBOMe-M (*N*-demethoxybenzyl-*O*-demethyl-) *N*-acetyl isomer 2 (R)**						7.72
	MS^1	PM at *m/z* 336.0086 (M+H)	23	336.0091	$C_{11}H_{15}O_3NI$	-1.56
	MS^2	FI at *m/z* 150.0677	42	150.0681	$C_9H_{10}O_2$	-2.53
		FI at *m/z* 209.1048	17	209.1052	$C_{11}H_{15}O_3N$	-1.88
		FI at *m/z* 261.9488	51	261.9491	$C_8H_7O_2I$	-1.08
		FI at *m/z* 276.9723	100	276.9726	$C_9H_{10}O_2I$	-0.93
		FI at *m/z* 293.9987	24	293.9991	$C_9H_{13}O_2NI$	-1.38
41	**25I-NBOMe-M (*O,O-bis*-demethyl-) *S*-methyl (H/R)**						8.18
	MS^1	PM at *m/z* 446.0278 (M+H)	11	446.0281	$C_{17}H_{21}O_3NIS$	-0.77
	MS^2	FI at *m/z* 121.0650	100	121.0653	C_8H_9O	-2.81
		FI at *m/z* 302.0973	1	302.0977	$C_{17}H_{18}O_3S$	-1.21
		FI at *m/z* 307.9358	4	307.9368	$C_9H_9O_2IS$	-3.26
		FI at *m/z* 322.9592	4	322.9603	$C_{10}H_{12}O_2IS$	-3.34
42	**25I-NBOMe-M (*O,O-bis*-demethyl-*bis*-HO-) *O*-methyl (H/R)**						7.72
	MS^1	PM at *m/z* 446.0473 (M+H)	9	446.0459	$C_{17}H_{21}O_5NI$	3.13
	MS^2	FI at *m/z* 137.0599	32	137.0603	$C_8H_9O_2$	-2.59
		FI at *m/z* 167.0703	100	167.0708	$C_9H_{11}O_3$	-3.11
		FI at *m/z* 262.9564	33	262.9569	$C_8H_8O_2I$	-1.93
43	**25I-NBOMe-M (*O*-demethyl-*bis*-HO-) *O*-methyl (H/R)**						7.01
	MS^1	PM at *m/z* 460.0624 (M+H)	0	460.0616	$C_{18}H_{23}O_5NI$	1.84
	MS^2	FI at *m/z* 137.0600	32	137.0603	$C_8H_9O_2$	-1.86
		FI at *m/z* 167.0707	100	167.0708	$C_9H_{11}O_3$	-0.72
		FI at *m/z* 276.9730	8	276.9726	$C_9H_{10}O_2I$	1.60
		FI at *m/z* 293.9990	4	293.9991	$C_9H_{13}O_2NI$	-0.36
44	**25I-NBOMe-M (*O,O,O-tris*-demethyl-) sulfate isomer 1 (R)**						5.79
	MS^1	PM at *m/z* 465.9823 (M+H)	21	465.9816	$C_{15}H_{17}O_6NIS$	1.52
	MS^2	FI at *m/z* 107.0496	100	107.0497	C_7H_7O	-0.84
		FI at *m/z* 262.9567	71	262.9569	$C_8H_8O_2I$	-0.79
		FI at *m/z* 342.9129	35	342.9137	$C_8H_8O_5IS$	-2.40
		FI at *m/z* 359.9395	83	359.9403	$C_8H_{11}O_5NIS$	-2.15
		FI at *m/z* 386.0250	11	386.0253	$C_{15}H_{17}O_3NI$	-0.83
45	**25I-NBOMe-M (*O,O,O-tris*-demethyl-) sulfate isomer 2 (R)**						6.14
	MS^1	PM at *m/z* 465.9825 (M+H)	27	465.9816	$C_{15}H_{17}O_6NIS$	1.95
	MS^2	FI at *m/z* 107.0496	100	107.0497	C_7H_7O	-0.84
		FI at *m/z* 262.9567	74	262.9569	$C_8H_8O_2I$	-0.79
		FI at *m/z* 342.9132	27	342.9137	$C_8H_8O_5IS$	-1.53
		FI at *m/z* 359.9396	64	359.9403	$C_8H_{11}O_5NIS$	-1.87

		FI at *m/z* 386.0250	18	386.0253	$C_{15}H_{17}O_3NI$	-0.83	
46	**25I-NBOMe-M (*bis*-HO-) *O*-methyl (H)**						8.05
	MS^1	PM at *m/z* 474.0781 (M+H)	0	474.0772	$C_{19}H_{25}O_5NI$	1.89	
	MS^2	FI at *m/z* 137.0600	31	137.0603	$C_8H_9O_2$	-1.86	
		FI at *m/z* 167.0705	100	167.0708	$C_9H_{11}O_3$	-1.92	
		FI at *m/z* 290.9881	18	290.9882	$C_{10}H_{12}O_2I$	-0.37	
		FI at *m/z* 308.0146	8	308.0148	$C_{10}H_{15}O_2NI$	-0.51	
47	**25I-NBOMe-M (*O,O-bis*-demethyl-) sulfate isomer 1 (H/R)**						6.54
	MS^1	PM at *m/z*479.9982 (M+H)	7	479.9972	$C_{16}H_{19}O_6NIS$	2.00	
	MS^2	FI at *m/z* 91.0549	27	91.0548	C_7H_7	1.37	
		FI at *m/z* 121.0653	100	121.0653	C_8H_9O	-0.33	
		FI at *m/z* 400.0409	5	400.0410	$C_{16}H_{19}O_3NI$	-0.18	
48	**25I-NBOMe-M (*O,O-bis*-demethyl-) sulfate isomer 2 (H/R)**						7.43
	MS^1	PM at *m/z* 479.9978 (M+H)	24	479.9972	$C_{16}H_{19}O_6NIS$	1.17	
	MS^2	FI at *m/z* 107.0496	100	107.0497	C_7H_7O	-0.84	
		FI at *m/z* 276.9725	84	276.9726	$C_9H_{10}O_2I$	-0.21	
		FI at *m/z* 356.9288	45	356.9294	$C_9H_{10}O_5IS$	-1.61	
		FI at *m/z* 373.9556	84	373.9559	$C_9H_{13}O_5NIS$	-0.86	
		FI at *m/z* 400.0407	12	400.0410	$C_{16}H_{19}O_3NI$	-0.68	
49	**25I-NBOMe-M (*O,O-bis*-demethyl-) sulfate isomer 3 (R)**						7.99
	MS^1	PM at *m/z* 479.9977 (M+H)	27	479.9972	$C_{16}H_{19}O_6NIS$	0.96	
	MS^2	FI at *m/z* 107.0496	87	107.0497	C_7H_7O	-0.84	
		FI at *m/z* 204.0331	4	204.0331	$C_7H_{10}O_4NS$	0	
		FI at *m/z* 276.9725	100	276.9726	$C_9H_{10}O_2I$	-0.21	
		FI at *m/z* 293.9987	34	293.9991	$C_9H_{13}O_2NI$	-1.38	
		FI at *m/z* 400.0407	71	400.0410	$C_{16}H_{19}O_3NI$	-0.68	
50	**25I-NBOMe-M (*O*-demethyl-) sulfate (H)**						8.12
	MS^1	PM at *m/z* 494.0138 (M+H)	6	494.0129	$C_{17}H_{21}O_6NIS$	1.84	
	MS^2	FI at *m/z* 91.0549	28	91.0548	C_7H_7	1.37	
		FI at *m/z* 121.0652	100	121.0653	C_8H_9O	-1.16	
		FI at *m/z* 397.0300	1	397.0301	$C_{17}H_{18}O_3I$	-0.18	
		FI at *m/z* 414.0568	8	414.0566	$C_{17}H_{21}O_3NI$	0.43	
51	**25I-NBOMe-M (*O,O-bis*-demethyl-) acetylcysteine (R)**						6.77
	MS^1	PM at *m/z* 561.0544 (M+H)	22	561.0551	$C_{21}H_{26}O_6N_2IS$	-1.23	
	MS^2	FI at *m/z* 121.0650	100	121.0653	C_8H_9O	-2.81	
		FI at *m/z* 288.0818	1	288.0820	$C_{16}H_{16}O_3S$	-0.75	
		FI at *m/z* 432.0126	7	432.0130	$C_{16}H_{19}O_3NIS$	-1.03	
		FI at *m/z* 455.0129	2	455.0138	$C_{14}H_{20}O_5N_2IS$	-1.92	
52	**25I-NBOMe-M (*O,O,O-tris*-demethyl-) glucuronide (R)**						4.62
	MS^1	PM at *m/z* 562.0571 (M+H)	47	562.0569	$C_{21}H_{25}O_9NI$	0.42	
	MS^2	FI at *m/z* 107.0496	68	107.0497	C_7H_7O	-0.84	
		FI at *m/z* 262.9567	100	262.9569	$C_8H_8O_2I$	-0.79	
		FI at *m/z* 386.0250	48	386.0253	$C_{15}H_{17}O_3NI$	-0.83	
		FI at *m/z* 456.0158	30	456.0155	$C_{14}H_{19}O_8NI$	0.56	
53	**25I-NBOMe-M (*O,O-bis*-demethyl-) glucuronide isomer 1 (H/R)**						5.35
	MS^1	PM at *m/z* 576.0731 (M+H)	35	576.0725	$C_{22}H_{27}O_9NI$	1.02	
	MS^2	FI at *m/z* 91.0549	30	91.0548	C_7H_7	1.37	
		FI at *m/z* 121.0653	100	121.0653	C_8H_9O	-0.33	
		FI at *m/z* 400.0408	25	400.0410	$C_{16}H_{19}O_3NI$	-0.43	
54	**25I-NBOMe-M (*O,O-bis*-demethyl-) glucuronide isomer 2 (H/R)**						6.42
	MS^1	PM at *m/z* 576.0733 (M+H)	46	576.0725	$C_{22}H_{27}O_9NI$	1.37	
	MS^2	FI at *m/z* 107.0496	60	107.0497	C_7H_7O	-0.84	
		FI at *m/z* 276.9724	100	276.9726	$C_9H_{10}O_2I$	-0.57	
		FI at *m/z* 293.9987	42	293.9991	$C_9H_{13}O_2NI$	-1.38	
		FI at *m/z* 400.0410	56	400.0410	$C_{16}H_{19}O_3NI$	0	
		FI at *m/z* 470.0311	22	470.0312	$C_{15}H_{21}O_8NI$	-0.20	

55	**25I-NBOMe-M (*O,O-bis*-demethyl-) glucuronide isomer 3 (H)**						6.57
	MS^1	PM at *m/z* 576.0736 (M+H)	52	576.0725	$C_{22}H_{27}O_9NI$	1.89	
	MS^2	FI at *m/z* 107.0497	55	107.0497	C_7H_7O	0	
		FI at *m/z* 276.9725	100	276.9726	$C_9H_{10}O_2I$	-0.21	
		FI at *m/z* 293.9988	42	293.9991	$C_9H_{13}O_2NI$	-1.04	
		FI at *m/z* 400.0410	46	400.0410	$C_{16}H_{19}O_3NI$	0	
		FI at *m/z* 470.0311	11	470.0312	$C_{15}H_{21}O_8NI$	-0.20	
56	**25I-NBOMe-M (*O*-demethyl-) glucuronide isomer 1 (H/R)**						7.09
	MS^1	PM at *m/z* 590.0888 (M+H)	30	590.0882	$C_{23}H_{29}O_9NI$	1.08	
	MS^2	FI at *m/z* 91.0549	33	91.0548	C_7H_7	1.37	
		FI at *m/z* 121.0653	100	121.0653	C_8H_9O	-0.33	
		FI at *m/z* 276.9727	1	276.9726	$C_9H_{10}O_2I$	0.52	
		FI at *m/z* 414.0568	31	414.0566	$C_{17}H_{21}O_3NI$	0.43	
57	**25I-NBOMe-M (*O*-demethyl-) glucuronide isomer 2 (H/R)**						7.25
	MS^1	PM at *m/z* 590.0887 (M+H)	40	590.0882	$C_{23}H_{29}O_9NI$	0.91	
	MS^2	FI at *m/z* 91.0549	33	91.0548	C_7H_7	1.37	
		FI at *m/z* 121.0653	100	121.0653	C_8H_9O	-0.33	
		FI at *m/z* 270.1254	1	270.1256	$C_{17}H_{18}O_3$	-0.72	
		FI at *m/z* 414.0567	34	414.0566	$C_{17}H_{21}O_3NI$	0.19	
58	**25I-NBOMe-M (*O*-demethyl-) glucuronide isomer 3 (H)**						7.83
	MS^1	PM at *m/z* 590.0887 (M+H)	50	590.0882	$C_{23}H_{29}O_9NI$	0.91	
	MS^2	FI at *m/z* 107.0496	100	107.0497	C_7H_7O	-0.84	
		FI at *m/z* 290.9881	45	290.9882	$C_{10}H_{12}O_2I$	-0.37	
		FI at *m/z* 308.0146	17	308.0148	$C_{10}H_{15}O_2NI$	-0.51	
		FI at *m/z* 414.0567	33	414.0566	$C_{17}H_{21}O_3NI$	0.19	
59	**25I-NBOMe-M (*O,O-bis*-demethyl-HO-) glucuronide isomer 1 (R)**						4.69
	MS^1	PM at *m/z* 592.0686 (M+H)	29	592.0674	$C_{22}H_{27}O_{10}NI$	1.98	
	MS^2	FI at *m/z* 107.0496	24	107.0497	C_7H_7O	-0.84	
		FI at *m/z* 137.0600	100	137.0603	$C_8H_9O_2$	-1.86	
		FI at *m/z* 416.0354	22	416.0359	$C_{16}H_{19}O_4NI$	-1.17	
60	**25I-NBOMe-M (*O,O-bis*-demethyl-HO-) glucuronide isomer 2 (H/R)**						5.59
	MS^1	PM at *m/z* 592.0685 (M+H)	53	592.0674	$C_{22}H_{27}O_{10}NI$	1.81	
	MS^2	FI at *m/z* 123.0444	82	123.0446	$C_7H_7O_2$	-1.67	
		FI at *m/z* 276.9725	100	276.9726	$C_9H_{10}O_2I$	-0.21	
		FI at *m/z* 293.9986	46	293.9991	$C_9H_{13}O_2NI$	-1.72	
		FI at *m/z* 299.0771	4	299.0767	$C_{13}H_{15}O_8$	1.35	
		FI at *m/z* 416.0357	17	416.0359	$C_{16}H_{19}O_4NI$	-0.45	
61	**25I-NBOMe-M (*O,O-bis*-demethyl-HO-) glucuronide isomer 3 (R)**						5.87
	MS^1	PM at *m/z* 592.0683 (M+H)	45	592.0674	$C_{22}H_{27}O_{10}NI$	1.47	
	MS^2	FI at *m/z* 107.0496	56	107.0497	C_7H_7O	-0.84	
		FI at *m/z* 292.9672	100	292.9675	$C_9H_{10}O_3I$	-0.93	
		FI at *m/z* 309.9937	46	309.9940	$C_9H_{13}O_3NI$	-1.04	
		FI at *m/z* 416.0355	65	416.0359	$C_{16}H_{19}O_4NI$	-0.93	
		FI at *m/z* 486.0261	12	486.0261	$C_{15}H_{21}O_9NI$	0	
62	**25I-NBOMe-M (*O,O-bis*-demethyl-HO-) glucuronide isomer 4 (H/R)**						6.27
	MS^1	PM at *m/z* 592.0689 (M+H)	31	592.0674	$C_{22}H_{27}O_{10}NI$	2.49	
	MS^2	FI at *m/z* 123.0444	100	123.0446	$C_7H_7O_2$	-1.67	
		FI at *m/z* 276.9726	23	276.9726	$C_9H_{10}O_2I$	0	
		FI at *m/z* 293.9990	20	293.9991	$C_9H_{13}O_2NI$	-0.36	
		FI at *m/z* 416.0351	12	416.0359	$C_{16}H_{19}O_4NI$	-1.89	
63	**25I-NBOMe-M (*O*-demethyl-HO-) glucuronide isomer 1 (H/R)**						6.21
	MS^1	PM at *m/z* 606.0839 (M+H)	27	606.0831	$C_{23}H_{29}O_{10}NI$	1.36	
	MS^2	FI at *m/z* 137.0600	100	137.0603	$C_8H_9O_2$	-1.86	
		FI at *m/z* 276.9726	6	276.9726	$C_9H_{10}O_2I$	0	
		FI at *m/z* 293.9989	4	293.9991	$C_9H_{13}O_2NI$	-0.70	
		FI at *m/z* 430.0521	20	430.0515	$C_{17}H_{21}O_4NI$	1.31	

		FI at *m/z* 470.0315	6	470.0312	$C_{15}H_{21}O_8NI$	0.65	
64	**25I-NBOMe-M (*O*-demethyl-HO-) glucuronide isomer 2 (H/R)**						6.50
	MS^1	PM at *m/z* 606.0838 (M+H)	31	606.0831	$C_{23}H_{29}O_{10}NI$	1.19	
	MS^2	FI at *m/z* 91.0549	35	91.0548	C_7H_7	1.37	
		FI at *m/z* 121.0653	100	121.0653	C_8H_9O	-0.33	
		FI at *m/z* 303.1467	4	303.1471	$C_{17}H_{21}O_4N$	-1.18	
		FI at *m/z* 430.0518	33	430.0515	$C_{17}H_{21}O_4NI$	0.61	
65	**25I-NBOMe-M (*O*-demethyl-HO-) glucuronide isomer 3 (H)**						6.66
	MS^1	PM at *m/z* 606.0840 (M+H)	44	606.0831	$C_{23}H_{29}O_{10}NI$	1.52	
	MS^2	FI at *m/z* 123.0444	83	123.0446	$C_7H_7O_2$	-1.67	
		FI at *m/z* 290.9881	100	290.9882	$C_{10}H_{12}O_2I$	-0.37	
		FI at *m/z* 308.0147	43	308.0148	$C_{10}H_{15}O_2NI$	-0.18	
		FI at *m/z* 430.0516	9	430.0515	$C_{17}H_{21}O_4NI$	0.15	
66	**25I-NBOMe-M (*O*-demethyl-HO-) glucuronide isomer 4 (H)**						7.30
	MS^1	PM at *m/z* 606.0839 (M+H)	34	606.0831	$C_{23}H_{29}O_{10}NI$	1.36	
	MS^2	FI at *m/z* 123.0444	100	123.0446	$C_7H_7O_2$	-1.67	
		FI at *m/z* 290.9880	28	290.9882	$C_{10}H_{12}O_2I$	-0.71	
		FI at *m/z* 308.0146	16	308.0148	$C_{10}H_{15}O_2NI$	-0.51	
		FI at *m/z* 430.0520	15	430.0515	$C_{17}H_{21}O_4NI$	1.08	
67	**25I-NBOMe-M (*O*-demethyl-HO-) glucuronide isomer 5 (H)**						7.92
	MS^1	PM at *m/z* 606.0843 (M+H)	66	606.0831	$C_{23}H_{29}O_{10}NI$	2.02	
	MS^2	FI at *m/z* 123.0444	100	123.0446	$C_7H_7O_2$	-1.67	
		FI at *m/z* 290.9881	98	290.9882	$C_{10}H_{12}O_2I$	-0.37	
		FI at *m/z* 308.0145	27	308.0148	$C_{10}H_{15}O_2NI$	-0.83	
		FI at *m/z* 430.0523	74	430.0515	$C_{17}H_{21}O_4NI$	1.78	
68	**25I-NBOMe-M (HO-) glucuronide isomer 1 (H)**						7.16
	MS^1	PM at *m/z* 620.1000 (M+H)	27	620.0987	$C_{24}H_{31}O_{10}NI$	2.05	
	MS^2	FI at *m/z* 109.0653	54	109.0653	C_7H_9O	0	
		FI at *m/z* 137.0601	100	137.0603	$C_8H_9O_2$	-1.13	
		FI at *m/z* 313.0921	19	313.0923	$C_{14}H_{17}O_8$	-0.78	
		FI at *m/z* 444.0689	5	444.0672	$C_{18}H_{23}O_4NI$	3.86	
69	**25I-NBOMe-M (HO-) glucuronide isomer 2 (H)**						7.46
	MS^1	PM at *m/z* 620.0995 (M+H)	28	620.0987	$C_{24}H_{31}O_{10}NI$	1.25	
	MS^2	FI at *m/z* 107.0496	18	107.0497	C_7H_7O	-0.84	
		FI at *m/z* 137.0600	100	137.0603	$C_8H_9O_2$	-1.86	
		FI at *m/z* 313.0920	32	313.0923	$C_{14}H_{17}O_8$	-1.10	
		FI at *m/z* 444.0668	6	444.0672	$C_{18}H_{23}O_4NI$	-0.87	

Table 3 General involvement of the CYP isoenzymes on the formation of the given 25I-NBOMe metabolites (+: metabolite formation; ++: most intense peak among the metabolites; -: no metabolite formation)

25I-NBOMe metabolite	CYP 1A2	CYP 2A6	CYP 2B6	CYP 2C8	CYP 2C9	CYP 2C19	CYP 2D6	CYP 2E1	CYP 3A4	CYP 3A5
N-demethoxybenzyl (**5**)	+	-	+	-	-	-	-	-	++	-
O-demethyl isomer 1 (**12**)	+	-	+	-	++	+	+	-	+	-
O-demethyl isomer 3 (**14**)	+	-	+	+	++	+	+	-	+	-
Hydroxy isomer 3 (**34**)	++	-	-	-	-	-	+	-	+	+
Hydroxy isomer 4 (**35**)	-	-	-	-	-	-	-	-	++	+

Table 4 25I-NBOMe and its metabolites, protonated precursor ions, characteristic MS^2 and MS^3 fragment ions, retention time (RT), and detectability in rat urine (RU) or human urine (HU) by LC-MS^n SUSA after 0.1 or 0.05 mg/kg BW dose. The numbers correspond to those of Tables 1 and 2.

No.	25I-NBOMe and its metabolites	Precursor ions, *m/z*	MS^2 fragment ions [*m/z*] and relative intensity, %	MS^3 fragment ions, *m/z*, and relative intensity, %, on the ion given in bold	RT, min	Detected in urine sample; dose given in brackets
1	25I-NBOMe	428	121 (8), 272 (100), 284 (12), 291 (7), 301 (8), 306 (6)	**272:** 121 (19), 135 (40), 151 (100), 225 (23), 241 (97)	16.04	RU (0.1)
12	25I-NBOMe-M (*O*-demethyl-) isomer 1	414	121 (18), 258 (17), 270 (100), 287 (29), 289 (30), 306 (19)	**270:** 133 (23), 149 (100), 162 (34), 239 (80)	14.97	HU
16	25I-NBOMe-M (*O,O-bis*-demethyl-HO-) isomer 2	416	277 (65), 294 (100)	**277:** 135 (54), 150 (100) **294:** 135 (21), 150 (93), 262 (100)	11.17	HU
29	25I-NBOMe-M (*O*-demethyl-HO-) isomer 5	430	276 (5), 291 (100), 308 (71)	**291:** 149 (36), 164 (78), 261 (100) **308:** 149 (8), 164 (16), 276 (100)	14.54	HU
50	25I-NBOMe-M (*O*-demethyl-) sulfate	494	270 (4), 397 (9), 414 (100)	**397:** 121 (46), 270 (100) **414:** 121 (27), 258 (17), 270 (100)	13.70	HU
53	25I-NBOMe-M (*O,O-bis*-demethyl-) glucuronide isomer 1	576	256 (14), 383 (8), 400 (100)	**256:** 148 (100) **400:** 121 (37), 256 (100), 275 (37)	8.34	RU (0.1) RU (0.05)
54	25I-NBOMe-M (*O,O-bis*-demethyl-) glucuronide isomer 2	576	277 (24), 294 (39), 400 (100), 470 (18)	**294:** 135 (12), 150 (42), 262 (100) **400:** 277 (36), 294 (100)	10.22	HU
55	25I-NBOMe-M (*O,O-bis*-demethyl-) glucuronide isomer 3	576	277 (33), 294 (51), 400 (100), 470 (19)	**294:** 135 (17), 150 (100), 262 (57) **400:** 277 (49), 294 (100)	10.61	HU
56	25I-NBOMe-M (*O*-demethyl-) glucuronide isomer 1	590	258 (4), 270 (5), 414 (100)	**414:** 121 (97), 258 (79), 270 (100), 292 (32)	12.24	RU (0.1) HU
57	25I-NBOMe-M (*O*-demethyl-) glucuronide isomer 2	590	258 (3), 270 (20), 397 (9), 414 (100)	**414:** 121 (27), 258 (22), 270 (100), 287 (31), 289 (33), 306 (24)	12.61	HU
61	25I-NBOMe-M (*O,O-bis*-demethyl-HO-) glucuronide isomer 3	592	293 (25), 310 (37), 416 (100), 486 (10)	**310:** 166 (14), 278 (100) **416:** 277 (6), 293 (58), 310 (100)	9.32	RU (0.1)
64	25I-NBOMe-M (*O*-demethyl-HO-) glucuronide isomer 2	606	286 (16), 303 (19), 430 (100)	**303:** 121 (19), 178 (100), 274 (55) **430:** 178 (17), 274 (20), 286 (100), 303 (65)	10.91	RU (0.1) RU (0.05)
65	25I-NBOMe-M (*O*-demethyl-HO-) glucuronide isomer 3	606	276 (30), 291 (100), 308 (83), 430 (70)	**291:** 149 (33), 164 (63), 261 (100) **308:** 149 (6), 164 (35), 276 (100)	11.75	HU
66	25I-NBOMe-M (*O*-demethyl-HO-) glucuronide isomer 4	606	276 (11), 291 (48), 308 (40), 430 (100)	**291:** 149 (22), 164 (97), 261 (100) **430:** 276 (5), 291 (100), 308 (74)	12.88	HU
69	25I-NBOMe-M (HO-) glucuronide isomer 2	620	288 (35), 313 (83), 444 (100)	**313:** 107 (8), 109 (8), 137 (100) **444:** 137 (75), 288 (100), 306 (16)	13.27	HU

Table 5 25I-NBOMe and its metabolites, calculated masses of their precursor ions, retention times (RT) recorded in rat urine after the given dose or human urine by LC-HR-MS/MS SUSA The numbers correspond to those of Tables 1 and 2 (D = detection of the accurate mass precursor ion in HR full scan, I = identification via HR full scan and MS^2)

No.	25I-NBOMe and its metabolites	Calculated exact masses of precursor ions, *m/z*	RT, min	Human urine	Rat urine 4 mg/kg BW	Rat urine 0.1 mg/kg BW	Rat urine 0.05 mg/kg BW
1	25I-NBOMe	428.0717	6.77	D	I	**I**	-
4	25I-NBOMe-M (*N*-demethoxybenzyl-deamino-HOOC-*O*-demethyl-)	306.9467	5.79	D	I	D	D
7	25I-NBOMe-M (*O,O-bis*-demethyl-) isomer 1	400.0404	5.16	D	I	D	D
8	25I-NBOMe-M (*O,O-bis*-demethyl-) isomer 2	400.0404	5.73	I	I	-	-
12	25I-NBOMe-M (*O*-demethyl-) isomer 1	414.0561	6.12	I	I	D	D
16	25I-NBOMe-M (*O,O-bis*-demethyl-HO-) isomer 2	416.0353	5.05	I	-	-	-
26	25I-NBOMe-M (*O*-demethyl-HO-) isomer 2	430.0510	5.62	I	I	-	-
44	25I-NBOMe-M (*O,O,O-tris*-demethyl-) sulfate isomer 1	465.9816	4.54	-	I	D	-
45	25I-NBOMe-M (*O,O,O-tris*-demethyl-) sulfate isomer 2	465.9816	4.73	D	I	-	-
47	25I-NBOMe-M (*O,O-bis*-demethyl-) sulfate isomer 1	479.9972	5.17	I	I	D	D
48	25I-NBOMe-M (*O,O-bis*-demethyl-) sulfate isomer 2	479.9972	5.73	D	-	-	-
50	25I-NBOMe-M (*O*-demethyl-) sulfate	494.0129	6.16	I	-	-	-
52	25I-NBOMe-M (*O,O,O-tris*-demethyl-) glucuronide	562.0569	4.03	-	I	D	D
53	25I-NBOMe-M (*O,O-bis*-demethyl-) glucuronide isomer 1	576.0725	4.45	D	I	**I**	D
54	25I-NBOMe-M (*O,O-bis*-demethyl-) glucuronide isomer 2	576.0725	5.10	D	I	D	D
55	25I-NBOMe-M (*O,O-bis*-demethyl-)	576.0725	5.20	D	-	-	-

	glucuronide isomer 3						
56	25I-NBOMe-M (*O*-demethyl-) glucuronide isomer 1	590.0882	5.52	I	I	D	D
57	25I-NBOMe-M (*O*-demethyl-) glucuronide isomer 2	590.0882	5.68	I	I	-	-
58	25I-NBOMe-M (*O*-demethyl-) glucuronide isomer 3	590.0882	5.98	D	I	-	-
61	25I-NBOMe-M (*O,O-bis*-demethyl-HO-) glucuronide isomer 3	592.0674	4.77	-	I	D	D
63	25I-NBOMe-M (*O*-demethyl-HO-) glucuronide isomer 1	606.0831	5.01	D	I	-	-
64	25I-NBOMe-M (*O*-demethyl-HO-) glucuronide isomer 2	606.0831	5.16	D	I	I	D
65	25I-NBOMe-M (*O*-demethyl-HO-) glucuronide isomer 3	606.0831	5.29	I	-	-	-
66	25I-NBOMe-M (*O*-demethyl-HO-) glucuronide isomer 4	606.0831	5.65	D	-	-	-
67	25I-NBOMe-M (*O*-demethyl-HO-) glucuronide isomer 5	606.0831	6.07	D	-	-	-
68	25I-NBOMe-M (HO-) glucuronide isomer 1	620.0987	5.58	D	-	-	-
69	25I-NBOMe-M (HO-) glucuronide isomer 1	620.0987	5.82	I	-	-	-

Legends to Figures:

Fig. 1 HR-MS/MS spectra, proposed structures (unclear *O*-demethylation or hydroxylation positions are indicated by tildes), and predominant fragmentation patterns of 25I-NBOMe and its phase I metabolites arranged according to precursor mass (PM)

Fig. 2 Structures of 25I-NBOMe (**1**) and potential products (**1a-c**) of the postulated rearrangement reaction

Fig. 3 HR-MS/MS spectra, proposed structures (unclear *O*-demethylation or hydroxylation positions are indicated by tildes), and predominant fragmentation patterns of 25I-NBOMe and its phase II metabolites arranged according to precursor mass (PM)

Fig. 4 Metabolic pathways of 25I-NBOMe in human (H) and rat (R). Phase II metabolites: glucuronides (G), sulfates (S), glutathione conjugates (GSH), acetyl conjugates (AC), *O*-methyl conjugates (ME). Undefined position of *O*-demethylation or hydroxylation indicated by tildes.

Fig. 5 Reconstructed ion chromatograms of the given exact masses indicating the identified metabolites in the human urine by LC-HR-MS/MS SUSA (peak numbering according to Tables 1 and 2)

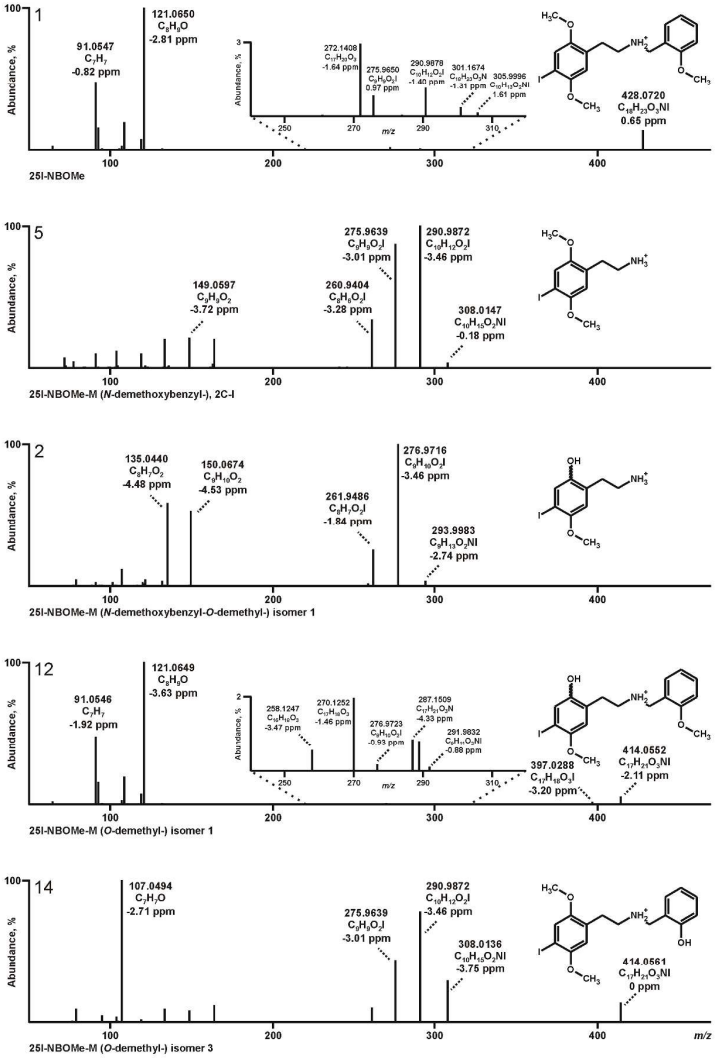

Fig. 1 HR-MS/MS spectra, proposed structures (unclear O-demethylation or hydroxylation positions are indicated by tildes), and predominant fragmentation patterns of 25I-NBOMe and its phase I metabolites arranged according to precursor mass (PM)

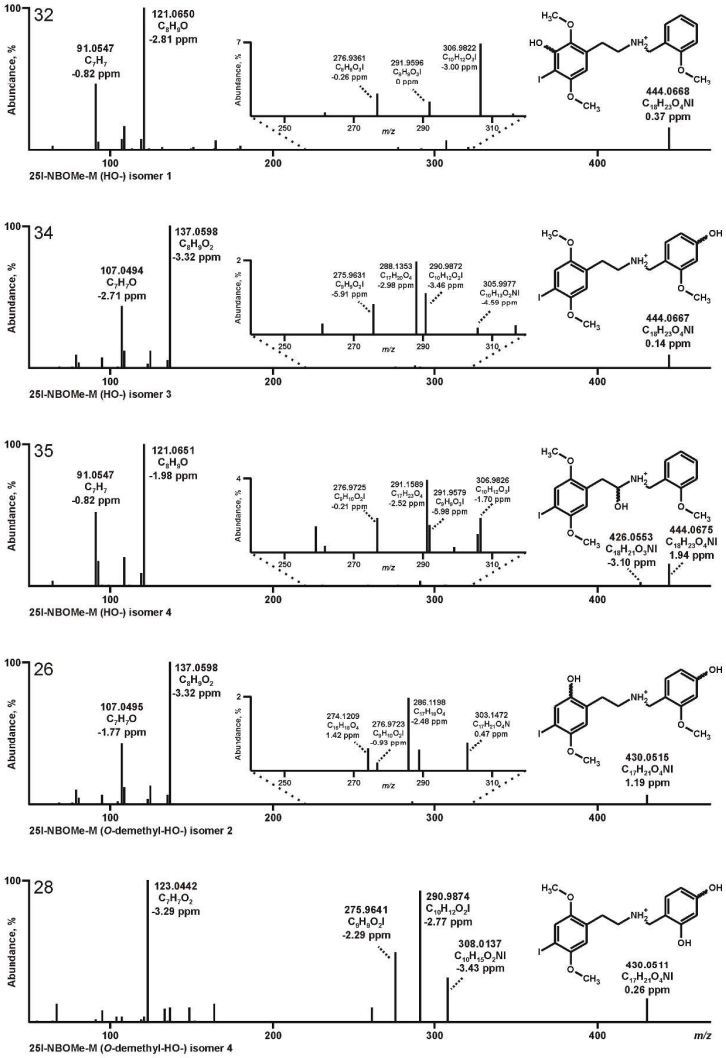

Fig. 1 continued

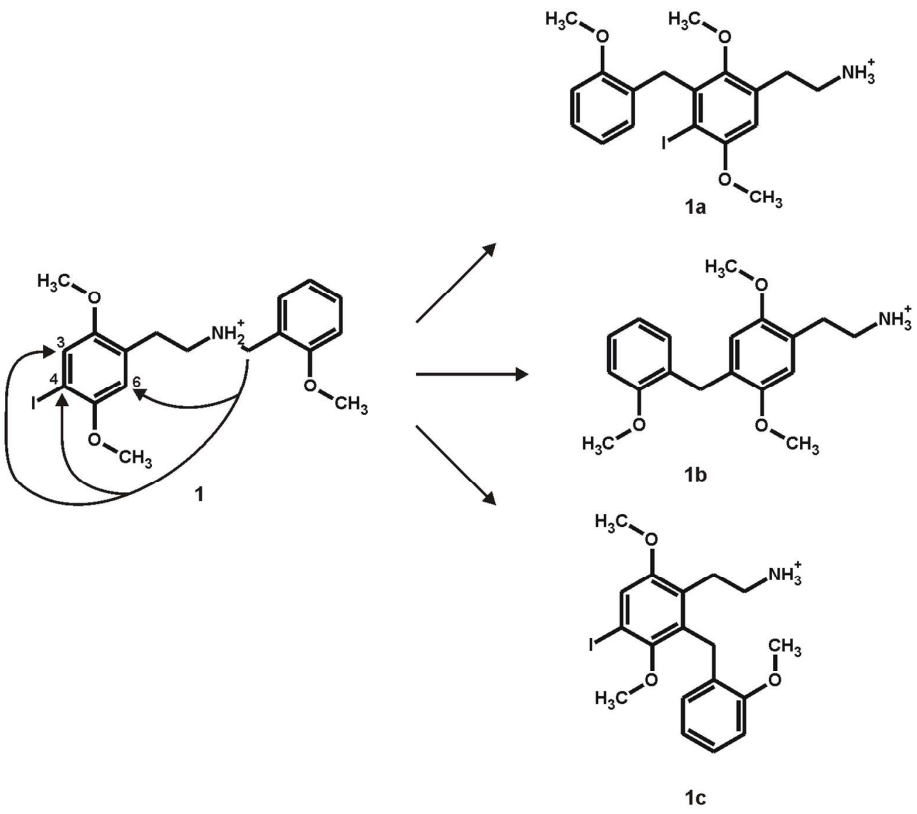

Fig. 2 Structures of 25I-NBOMe (1) and potential products (1a-c) of the postulated rearrangement reaction

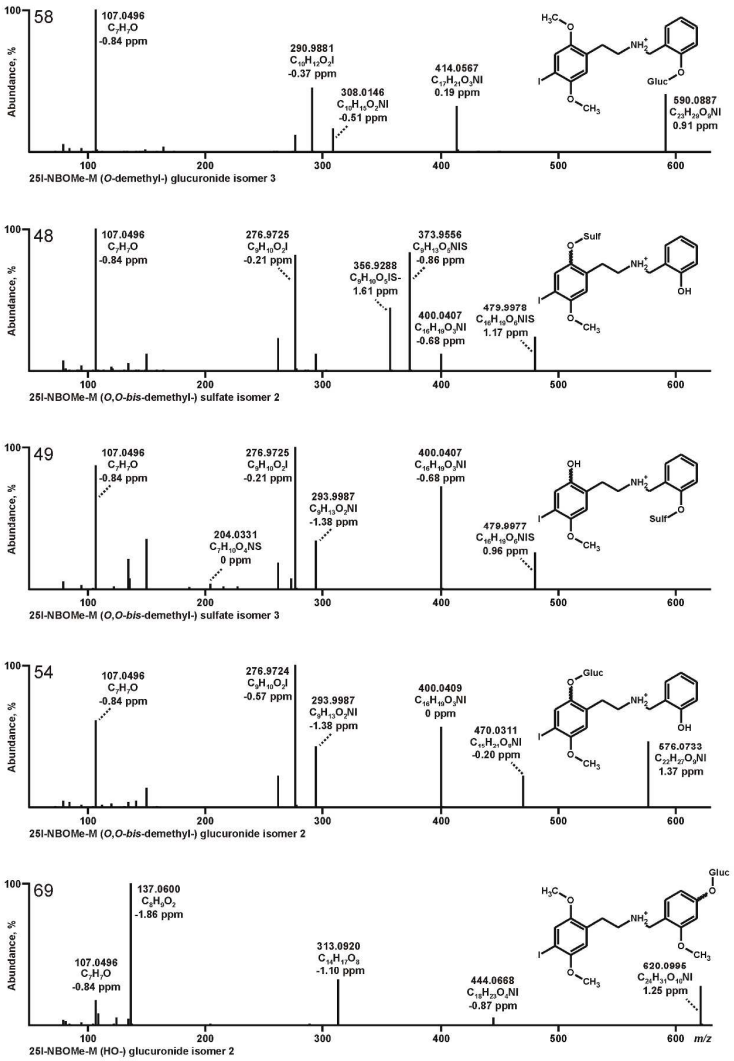

Fig. 3 HR-MS/MS spectra, proposed structures (unclear O-demethylation or hydroxylation positions are indicated by tildes), and predominant fragmentation patterns of 25I-NBOMe and its phase II metabolites arranged according to precursor mass (PM)

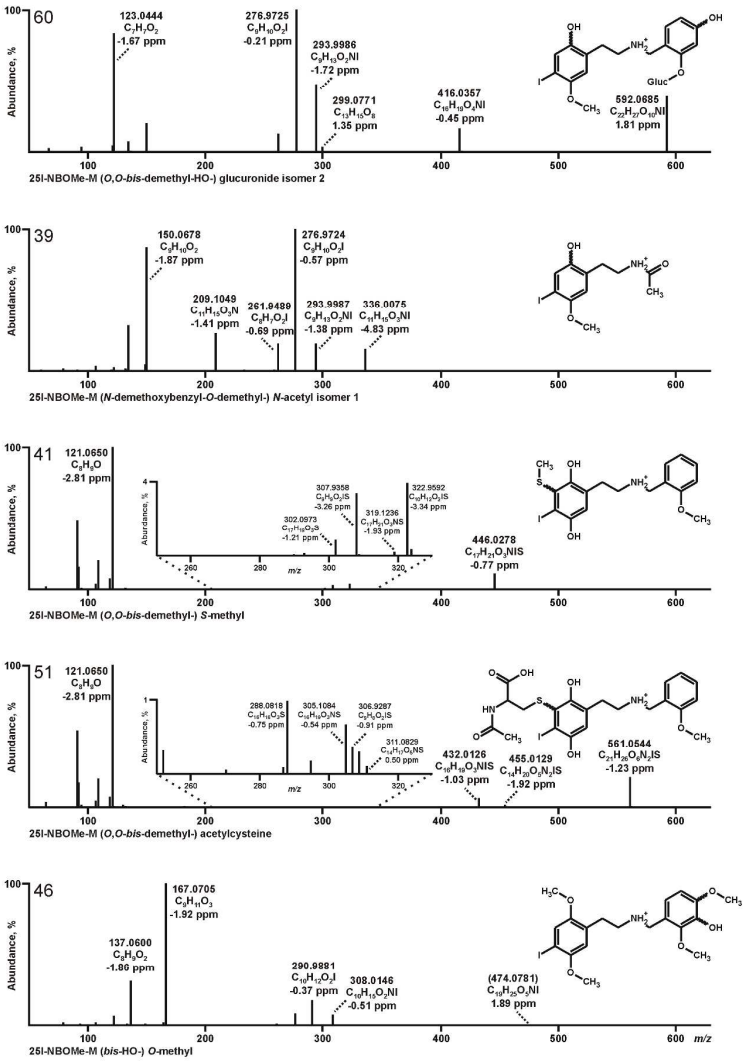

Fig. 3 continued

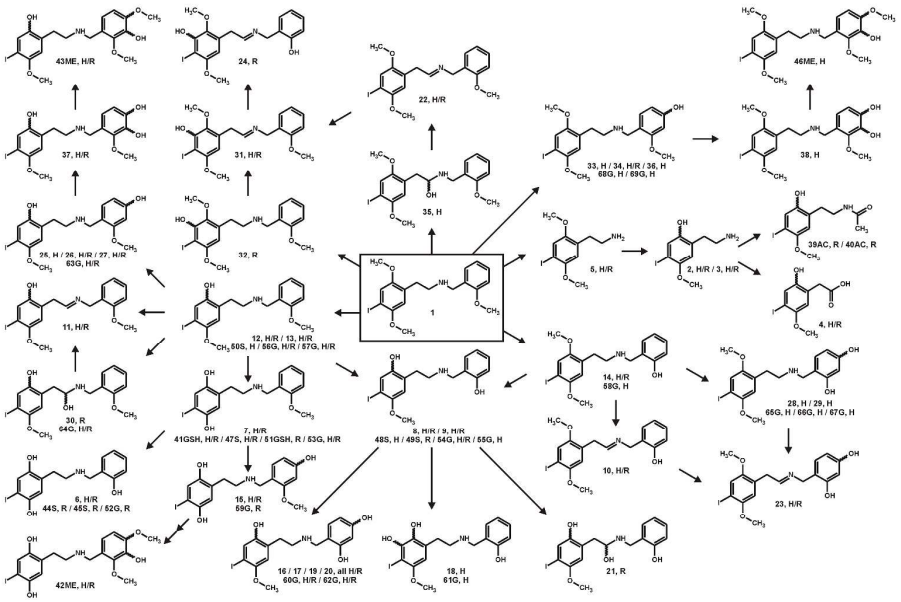

Fig. 4 Metabolic pathways of 25I-NBOMe in human (H) and rat (R). Phase II metabolites: glucuronides (G), sulfates (S), glutathione conjugates (GSH), acetyl conjugates (AC), O-methyl conjugates (ME). Undefined position of O-demethylation or hydroxylation indicated by tildes

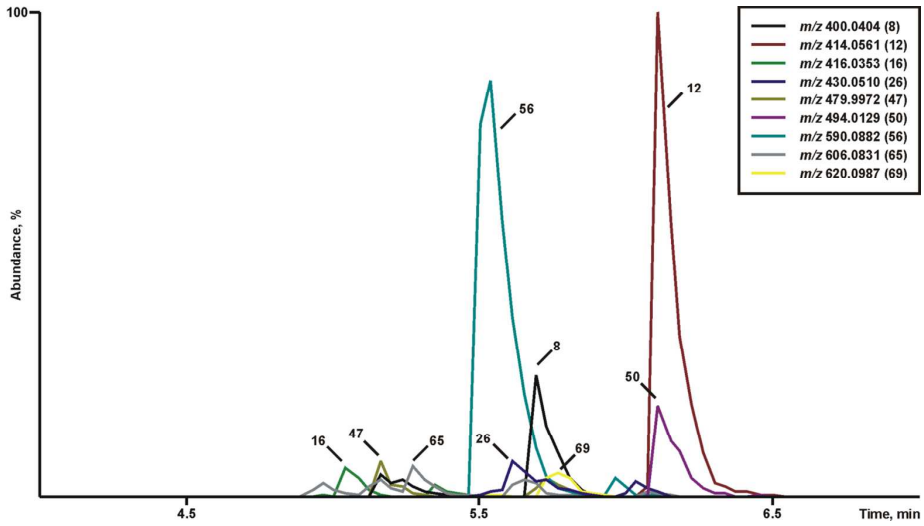

Fig. 5 Reconstructed ion chromatograms of the given exact masses indicating the identified metabolites in the human urine by LC-HR-MS/MS SUSA (peak numbering according to Tables 1 and 2)
343x193mm (122 x 122 DPI)